AD-A075 804 NORTH CAROLINA UNIV AT CHAPEL HILL DEPT OF CHEMISTRY F/G 20/3
MAGNETISM OF MIXED VALENCE COMPOUNDS.(U)
OCT 79 W E HATFIELD N00014-76-C-0816
UNCLASSIFIED TR-8 NL

END
DATE FILMED
11-79
DDC

(12)

OFFICE NAVAL RESEARCH

(15) Contract N00014-76-C-0816-Mod. 4

Project .NR 053-617

(14) TR-

(9) TECHNICAL REPORT, NO. 8

(6) Magnetism of Mixed Valence Compounds*

by

(10) William E. Hatfield

(11) 1 Oct 79

(12) 54

Prepared for Publication

in

The Proceedings of a NATO Advanced Study Institute on Mixed Valence Compounds
Reidel Publishing Co. 1979

University of North Carolina
Department of Chemistry
Chapel Hill, North Carolina

October 1, 1979

Approved for Public Release: Distribution Unlimited.

400 342

SECURITY CLASSIFICATION OF THIS PAGE (When Data Entered)

REPORT DOCUMENTATION PAGE		READ INSTRUCTIONS BEFORE COMPLETING FORM
1. REPORT NUMBER 8	2. GOVT ACCESSION NO.	3. RECIPIENT'S CATALOG NUMBER
4. TITLE (and Subtitle) Magnetism of Mixed Valence Compounds		5. TYPE OF REPORT & PERIOD COVERED
		6. PERFORMING ORG. REPORT NUMBER
7. AUTHOR(s) William E. Hatfield		8. CONTRACT OR GRANT NUMBER(s) N0014-76-C-0816-Mod. 4
9. PERFORMING ORGANIZATION NAME AND ADDRESS Department of Chemistry University of North Carolina Chapel Hill, NC 27514		10. PROGRAM ELEMENT, PROJECT, TASK AREA & WORK UNIT NUMBERS NR 053-617
11. CONTROLLING OFFICE NAME AND ADDRESS Office of Naval Research Department of the Navy Arlington, Virginia 22217		12. REPORT DATE October 1, 1979 13. NUMBER OF PAGES 51
14. MONITORING AGENCY NAME & ADDRESS(if different from Controlling Office)		15. SECURITY CLASS. (of this report) Unclassified 15a. DECLASSIFICATION/DOWNGRADING SCHEDULE

15. DISTRIBUTION STATEMENT (of this Report)

Approved for Public Release, Distribution Unlimited

17. DISTRIBUTION STATEMENT (of the abstract entered in Block 20, if different from Report)

18. SUPPLEMENTARY NOTES

To be published in the Proceedings of the NATO Advanced Study Institute on Mixed Valence Compounds, Reidel Publishing, Co. 1979.

19. KEY WORDS (Continue on reverse side if necessary and identify by block number)

Magnetic Susceptibilities, Crystal Structures, Mixed Valence Compounds, Antisymmetric Exchange, Anisotropic Exchange, Random Exchange, Metamagnetism, Electrical Conductivities, Intervalence Transitions, Electron Delocalization, Organometallic Compounds, Cubane Cluster Compounds; Linear Chain Compounds, Prussian Blue, Krogmann's Salt.

20. ABSTRACT (Continue on reverse side if necessary and identify by block number)

Results of representative studies of magnetic properties of mixed valence compounds are described in terms of Heisenberg-Van Vleck-Direc exchange theory, which is developed. Systems of discrete clusters, chains, sheets, and three dimensional polymeric materials are discussed. Several important problems requiring additional research are identified.

DD FORM 1 JAN 73 1473 EDITION OF 1 NOV 65 IS OBSOLETE

SECURITY CLASSIFICATION OF THIS PAGE (When Data Entered)

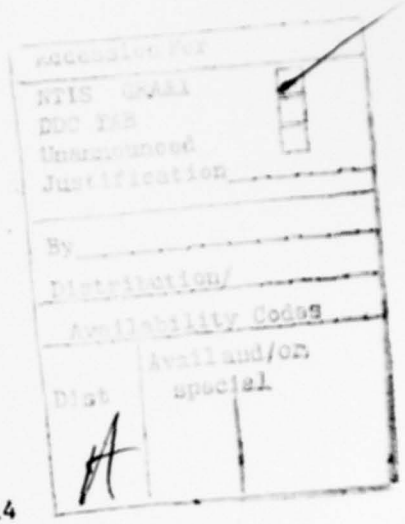

MAGNETISM OF MIXED VALENCE COMPOUNDS

William E. Hatfield

Department of Chemistry
University of North Carolina
Chapel Hill, North Carolina 27514

Mixed valence compounds exhibit a wide range of magnetic properties. These properties range from simple diamagnetism which is temperature independent and which may be estimated rather accurately from Pascal's constants, to Curie-Weiss paramagnetism, to exceptionally complicated behavior which may arise from single ion effects, exchange coupling interactions, or both. Studies of the magnetic properties of mixed valence compounds often yield valuable information concerning the chemical nature and electronic structure of the substances. In this chapter, results of representative studies of magnetic properties of mixed valence compounds will be described with the aim of illustrating the phenomena which are exhibited and the manner in which the results are used in the solution of chemical problems. Systems of discrete clusters, chains, sheets, and three dimensional polymeric materials will be discussed here. For the most part, these will be compounds in which metal ions are bridged by ligands such as halides, oxide, pyrazine, and other ions and small molecules, although representative results for compounds containing metal-metal bonds will be included. Because of space limitations and a recent review[1] on the subject, results on mixed valence metalloproteins and enzymes will not be covered.

Since the magnetic properties of mixed valence compounds which contain paramagnetic metal ions that are not exchange coupled, or involved in rapid electron transfer, or delocalized, may be understood in terms of the appropriate theories for single ion molecular species, and since this is a complete topic in itself, class I systems in the Robin and and Day[2] scheme will not be discussed here.

SURVEY OF THEORETICAL RESULTS

Much of the theory necessary for the analysis of the magnetic properties of mixed valence compounds is the same as that used for compounds in which all paramagnetic species are in the same formal oxidation state. For discrete clusters, the general approach described by Kambe[3] is usually followed, although the technique becomes very tedious when the number of paramagnetic species becomes large and the symmetry of the cluster decreases.[4] Additional complications arise for mixed valence complexes especially if these involve random mixtures of spins. Kudo, Matsubara, and Katsura have discussed the expected magnetic behavior of random mixtures of $S = 1/2$, $S = 0$ and $S = 1/2$, $S = 1$ ions within a statistical framework,[5] and Wrobleski and Brown have illustrated the problems in their study of mixed valence iron oxalate, squarate, and dihydroxybenzoquinone coordination polymers.[6] Random exchange in linear chains has been the subject of extensive studies and results are discussed in a subsequent section.

Theoretical studies of polymeric materials have provided several exact solutions which are valuable for the analysis of magnetic data. These results include the one-dimensional Ising chain,[7] the two-dimensional Ising layer,[8] the one-dimensional XY chain,[9] and the one-dimensional Heisenberg chain with infinite spin.[10] Results of calculations using various degrees of approximations are also available for several other systems. Bonner and Fisher[11] have carried out exact calculations on short chains of $S = 1/2$ Heisenberg spins and have extrapolated their results to the infinite one-dimensional limit. Weng,[12] using a similar procedure, has calculated the magnetic properties of linear Heisenberg chains with $S \geq 1$. Wagner and Friedberg[13] have shown that the infinite spin model of Fisher can be scaled to the exact results[14] of the high temperature series expansion for the limiting case of large spins, e.g. $S = 5/2$. Development of additional models has been presented by Smart,[15] and the application of the results to chemical systems has been critically reviewed by DeJongh and Miedema.[16]

Curie-Weiss Law. We will begin our discussion by considering the Curie-Weiss law. In equation (1), χ is field independent

$$\chi = C/(T-\theta) \qquad (1)$$

paramagnetic susceptibility, C is the Curie constant, T is the temperature, and θ is the Weiss constant. Severe deviations of experimental data from the Curie-Weiss law signal electronic state complexities, and in favorable cases it is possible to develop a model which accounts for the deviation, thereby suggesting an explanation for the phenomena that give rise to the deviation.

Let us assume that the deviations arise from exchange interactions, in which case the effective magnetic field $\underline{H}$ (effective) is the sum of the applied, external magnetic field $\underline{H}$ (external) plus the internal magnetic field. The internal magnetic field $\underline{H}$ (internal) is related to the magnetization by the molecular field constant γ. That is, $\underline{H}$ (internal) = $\gamma\underline{M}$, and $\underline{H}$ (effective) = $\underline{H}$ (external) + $\gamma\underline{M}$. Magnetization is given by

$$\underline{M} = Ng^2\mu_B^2 J(J+1)\underline{H}/3kT \qquad (2)$$

where J is the total angular momentum quantum number and the other symbols have their usual meaning. Substitution of $\underline{H}$ (effective) in equation (2) for $\underline{H}$ yields $\underline{M} = C[\underline{H}\text{ (external)} + \gamma\underline{M}]/T$, from which C, the Curie constant, is given by $Ng^2\mu_B^2 J(J+1)/3k$. Since $\underline{M} = \chi\underline{H}$ (external), then $\chi = C/(T-\gamma C) = C/(T-\theta)$. The sign of θ may be positive or negative depending on the nature of the exchange interactions being negative for antiferromagnetic interactions and positive for ferromagnetic interactions, and the magnitude of θ is a gauge of the strength of these interactions.

The Heisenberg-Dirac-Van Vleck Hamiltonian. The Hamiltonian that is used as the starting point in discussion of exchange theory for systems with unpaired electrons localized on the paramagnetic ions is

$$\underline{H} = -2 \sum_{n<m} J_{nm}\hat{\underline{S}}_n \cdot \hat{\underline{S}}_m \qquad (3)$$

where the summation is overall paramagnetic ions in the system under consideration, J_{nm} is the exchange integral between ions n and m, and $\underline{S}_n$ and $\underline{S}_m$ spin angular momentum operators. In the Heisenberg-Dirac-Van Vleck model it is assumed that the interacting ions are orbitally nondegenerate, that any orbital contribution will be accommodated in the parametrized g value, and usually nearest neighbor interactions only are considered. Almost always J_{ij} is taken to be isotropic. In a magnetic field the term $-g\mu_B\sum_i(\hat{L}_i + 2\hat{S}_i)\cdot\underline{H}$ must be added to the Hamiltonian.

The development of the theory for two interacting indistinguishable particles, say electrons in orbitals ψ^a and ψ^b on centers a and b, illustrates the approach to the theoretical description of the problem. The wave equation for two noninteracting electrons takes the form $[\underline{H}_1 + \underline{H}_2]\psi^a_{(1)}\psi^b_{(2)} = [E_a + E_b]\psi^a_{(1)}\psi^b_{(2)}$ where $\underline{H}_1$ operates only on $\psi_{(1)}$ and $\underline{H}_2$ operates only on $\psi_{(2)}$, and the energy eigenvalue is two fold degenerate because the electrons are indistinguishable. The degeneracy is lifted when the Coulomb interactions between the electrons and nuclei are taken into consideration by addition of the term

$H' = e^2/R_{ab} + e^2/r_{12} - e^2/r_{a2} - e^2/r_{b1}$ to the Hamiltonian. Using perturbation theory, the secular determinantal equation

$$\begin{vmatrix} |\psi_1\rangle & |\psi_2\rangle \\ H'_{11}-E & H'_{12}-ES \\ H'_{21}-ES & H'_{22}-E \end{vmatrix} = 0$$

must be solved. Here $\psi_1 = \psi^a(1)\psi^b(2)$ and $\psi_2 = \psi^a(2)\psi^b(1)$, $H = H_1 + H_2 + H'$, and $H_{ij} = \int \psi_i^* H \psi_j d\tau$. By definition,

$$J_{ab} = H'_{12} = H'_{21} = \int \psi_a^*(1)\psi_b^*(2)\{H'\}\psi_b(1)\psi_a(2)d\tau_1 d\tau_2.$$

$$K_{ab} = H'_{11} = H'_{22} = \int \psi_{a(1)}^*\psi_b^*(2)\{H'\}\psi_{a(1)}\psi_{b(2)}d\tau_1 d\tau_2.$$

$$= \int \psi_{a(2)}^*\psi_{b(1)}^*\{H'\}\psi_{a(2)}\psi_{b(1)}d\tau_1 d\tau_2.$$

The eigenvalues are $E_\pm = E_a + E_b + (K \pm J)/(1 \pm S)$ where S is the overlap integral, and the eigen functions are the symmetric and antisymmetric combinations

$$\psi_{sym} = [\psi_{a(1)}\psi_{b(2)} + \psi_{a(2)}\psi_{b(1)}]/\sqrt{2}$$

$$\psi_{anti} = [\psi_{a(1)}\psi_{b(2)} - \psi_{a(2)}\psi_{b(1)}]/\sqrt{2}$$

If we ignore the overlap integral, then the energy difference between these two eigenstates is 2J. Up to this point, the spin coordinates have been left out to emphasize the fact that exchange is an electrostatic orbital interaction. However, the total wave function must be a product of the orbital part and a spin part.

Now consider the spin properties. Each electron has spin angular momentum $\hbar/2$, and by the vector addition rule the total spin of the system may be either S = 1 (triplet state) or S = 0 (singlet state). For the triplet state, the possible values for the z component of the total spin are 1, 0, -1. If, in the usual manner, $\alpha = +1/2$ and $\beta = -1/2$, then the spin functions $|S,M_s\rangle$ are

$$|1,1\rangle = |\alpha_1\alpha_2\rangle$$

$$|1,0\rangle = [|\alpha_1\beta_2\rangle + |\beta_1\alpha_2\rangle]/\sqrt{2}$$

$$|1,-1\rangle = |\beta_1\beta_2\rangle$$

and

$$|0,0\rangle = [|\alpha_1\beta_2\rangle - |\beta_1\alpha_2\rangle]/\sqrt{2}$$

where the triplet state spin functions are symmetric and the singlet state spin function is antisymmetric.

According to the Pauli principle the total wave function must be antisymmetric with respect to exchange of every pair of electrons. Therefore, the symmetric spin functions (triplet state) must be combined with the ψ_{anti}, and the antisymmetric spin function (singlet state) must be combined with ψ_{sym}. It is in this way that the energy of the system depends on the total spin.

In terms of a vector model, we take $\underline{s}_1$ and $\underline{s}_2$ to be the spin angular momentum operators in units of $\hbar$ with the vector sum $\underline{s}_{12} = \underline{s}_1 + \underline{s}_2$, and

$$(\underline{s}_{12})^2 = (\underline{s}_1 + \underline{s}_2)^2 = (\underline{s}_1)^2 + (s_2)^2 + 2s_1 \cdot s_2$$

The eigenvalues of the operators $\underline{s}_{12}{}^2$, $s_1{}^2$, and $s_2{}^2$ are $S(S+1)$, $s_1(s_1+1)$, and $s_2(s_2+1)$. Application of the operator $\underline{s}_1 \cdot \underline{s}_2 = 1/2[(\underline{s}_{12})^2 - (s_1)^2 - (s_2)^2]$ yields:

$$\text{for } S = 1,\ \underline{S}_1 \cdot \underline{S}_2 = 1/2[1(1+1) - 1/2(1/2+1) - 1/2(1/2+1)] = 1/4$$

$$\text{for } S = 0,\ \underline{S}_1 \cdot \underline{S}_2 = 1/2[0(0+1) - 1/2(1/2+1) - 1/2(1/2+1)] = -\frac{3}{4}$$

This permits us to write the exchange Hamiltonian as $H' = -2J\hat{\underline{S}}_1 \cdot \hat{\underline{S}}_2$. For the multielectron case where for atom a the total spin is $\underline{S}_a = \Sigma \underline{s}_i$, and for atom b, $S_b = \Sigma \underline{s}_j$ (where i and j denote the electrons on a and b, respectively), then we may write $H = -2J_{ab}\hat{\underline{S}}_a \cdot \hat{\underline{S}}_b$. For a cluster of exchange coupled ions we generalize to the Hamiltonian $H = -2 \sum_{n<m} J_{nm}\underline{S}_n \cdot \hat{\underline{S}}_m$, which was given at the beginning of this section.

Energy Levels in Exchange Coupled Clusters. Van Vleck has developed a convenient formula for the spin states which result from exchange interactions in clusters with n magnetically equivalent paramagnetic ions.[17] For the assembly of n spins, in the vector model, the resultant spin vector is $\underline{S}' = \Sigma_n \underline{S}_i$, with the square of $\underline{S}'$ being

$$[S']^2 = [\sum_{i=1}^{n} \underline{S}_i]^2 = \sum_{i=1}^{n} [\underline{S}_i]^2 + \sum_{i,j} \underline{S}_i \cdot \underline{S}_j$$

In the dot product the indices i and j designate adjacent paramagnetic ions. Combined with the results $[\underline{S}']^2 = S'(S'+1)$ and $[\underline{S}_i]^2 = S_i(S_i+1)$, and the realization that there are n terms in

$\Sigma[\underline{S}_i]^2$ and $n(n-1)$ terms in the dot product summation, we may write

$$\underline{S}_i \cdot \underline{S}_j = \frac{S'(S'+1) - nS_i(S_i+1)}{n(n-1)}$$

since all spins are equivalent. There are n(n-1)/2 terms in the Hamiltonian $H = -2J \sum_{i \neq j} \underline{S}_i \cdot \underline{S}_j$. The energies of the spin states are given by

$$E(S') = -J[S'(S'+1) - nS_i(S_i+1)] \qquad (4)$$

where S' can take the values allowed by the vector summation rule. For $n = 2$, $S' = 0,1$; for $n = 3$, $S' = 1/2, 3/2$; for $n = 4$, $S' = 0,1,2$.

It is clear that more than one spin state with a given S' may arise. Van Vleck[17] has shown that the number of states W with a given S' is given by

$$W(S') = \Omega(S') - \Omega(S'+1) \qquad (5)$$

where $\Omega(S')$ is the coefficient of $X^{S'}$ in the expansion of

$$(X^S + X^{S-1} + \ldots + X^{-S})^n$$

Consider for example an assembly of three paramagnetic ions with $S_i = 1/2$. The expression to be expanded is $(X^{1/2} + X^{-1/2})^3$, which gives $X^{3/2} + 3X^{1/2} + \ldots$, and the number of states with $S' = 3/2$ is 1 while the number with $S' = 1/2$ is 2. If all interacting ions are magnetically equivalent then all states of a given S' are degenerate.

The Van Vleck Equation. In the magnetic susceptibility experiment, one measures the bulk property as a function of temperature and magnetic field strength, and analyzes the data in terms of the distribution of energy levels which are thermally populated. Usually the energies of these levels are not known, but frequently their relative energies in terms of pertinent parameters, say exchange coupling constants, are known. In such cases appropriate theoretical equations are fit to the experimental data to yield the desired parameters. The most widely used formalism was developed by Van Vleck.

By definition, the magnetic moment $\mu_{n,m}$ of an energy level $E_{n,m}$ is given by $\mu_{n,m} = -\partial E_{n,m}/\partial H$, where H is the magnetic field. The total moment of the system, M is

$$M_i = \frac{N\sum_{n,m} \mu_{n,m} \exp(-E_{n,m}/kT)}{\sum_{n,m} \exp(-E_{n,m}/kT)} \qquad (i = x,y,z)$$

where N is Avogadro's number, and the summation is over all states. Consider one of these states: The energy of the nth state can be expressed in terms of a power series in H as

$$E_{n,m} = E^{\circ}_{n,m} + HE^{(1)}_{n,m} + H^2E^{(2)}_{n,m} + \ldots$$

where $E^{o}_{n,m}$ is the zero field energy and $E^{(1)}_{n,m}$, $E^{(2)}_{n,m}$, ... are the first, second,... Zeeman coefficients. The moment of this state is

$$\mu_{n,m} = -E^{(1)}_{n,m} - 2E^{(2)}_{n,m}H - \ldots$$

It is convenient to expand the exponent

$$\exp(-E_{n,m}/kT) = \exp\left(\frac{-E^{\circ}_{n,m} - HE^{(1)}_{n,m} - H^2E^{(2)}_{n,m} \ldots}{kT}\right)$$

$$\approx \left[1 - \frac{HE^{(1)}_{n,m}}{kT}\right] \exp\left(\frac{-E^{\circ}_{n,m}}{kT}\right)$$

and to express the total moment as

$$M_i = \frac{N\sum_{n,m}(-E^{(1)}_{n,m} - 2HE^{(2)}_{n,m} - \ldots)(1-HE^{(1)}_{n,m}/kT)\exp(-E^{\circ}_{n,m}/kT)}{\sum_{n,m}(1-HE^{(1)}_{n,m}/kT)\exp(-E^{\circ}_{n,m}/kT)}$$

Paramagnetic substances do not possess magnetic moments in the absence of magnetic fields, so

$$\sum_{n,m}[\{-E^{(1)}_{n,m}\}\exp(-E^{\circ}_{n,m}/kT)] = 0$$

If data are collected at moderate temperatures and magnetic fields then only first order terms in H in the numerator and terms independent of H in the denominator need be retained. By definition $\chi_i = M_i/H_i$, and we have the Van Vleck equation:

$$\chi_i = \frac{N\sum_{n,m}[(E^{(1)}_{n})^2/kT - 2E^{(2)}_{n,m}]\exp(-E^{\circ}_{n,m}/kT)}{\sum_{n,m}\exp(-E^{\circ}_{n,m}/kT} \qquad (6)$$

This equation will be utilized frequently in the section on Representative Results.

Anisotropic and Antisymmetric Exchange. Frequently, the exchange Hamiltonian $H = -2\sum_{n<m} J_{nm}\underline{S}_n \cdot \underline{S}_m$ cannot adequately explain

experimental data, and it is necessary to consider additional kinds of interactions. The Hamiltonian as written above implies that the exchange interactions are isotropic and symmetric. If we rewrite the Hamiltonian as

$$H_{nm} = -2\sum_{n<m} J_{nm}\{\hat{S}_{1z}\hat{S}_{2z} + \alpha(\hat{S}_{1x}\hat{S}_{2x} + \hat{S}_{1y}\hat{S}_{2y})\}$$

the multiplier α can be used to account for axial anisotropic symmetric exchange interactions. The Heisenberg case arises when $\alpha = 1$, the Ising case results when $\alpha = 0$, and there are experimental examples for both extreme cases as well as for intermediate values of α, that is, for $0 < \alpha < 1$.

It is instructive to examine the Ising case in detail, and we will use as our example the pair of $S = 1/2$ exchange coupled ions for which the spin wave functions were given above. The exchange coupling operator for this case is $H = -2J_{12}^{z}\hat{S}_{1z}\hat{S}_{2z}$. Applying the operator to the basis set yields the determinantal equation

$$\begin{vmatrix} |\alpha\alpha\rangle & |\alpha\beta+\beta\alpha\rangle/\sqrt{2} & |\beta\beta\rangle & |\alpha\beta-\beta\alpha\rangle/\sqrt{2} \\ -\frac{1}{2}J_{12}^{z}-E & 0 & 0 & 0 \\ 0 & 1/2J_{12}^{z}-E & 0 & 0 \\ 0 & 0 & -1/2J_{12}^{z}-E & 0 \\ 0 & 0 & 0 & 1/2J_{12}^{z}-E \end{vmatrix} = 0$$

with two roots $E = +J_{12}^{z}$ and two roots $E = -J_{12}^{z}$. The energy separation between the two doublet states is $|J_{12}^{z}|$.

Frequently anisotropic exchange is taken into account by adding the term $\underline{S}_n \cdot \underline{\underline{\Gamma}}_{nm} \cdot \underline{S}_m$ to the Hamiltonian. In this term $\underline{\underline{\Gamma}}_{nm}$ is a symmetric tensor, and is given approximately by $(\Delta g/g)^2 J_{nm}$ where $\Delta g = |g-2|$. The effect of anisotropic exchange is to cause a zero-field splitting of the triplet state. In axial cases a singlet and doublet result, while all degeneracy is lifted in rhombic cases.

Antisymmetric exchange interactions may arise between pairs of exchange coupled ions when the single ion g values are different, a condition which implies that the exchange coupled ions are not related by a center of inversion. The term, which is added to the Hamiltonian to account for antisymmetric exchange is $\underline{D}_{nm} \cdot [\underline{S}_n \times \underline{S}_m]$, was theoretically established by Moriya following

a phenomenological development by Dzialoshinski. Essentially, this interaction tends to align the spins perpendicular to each other, and in this manner tends to oppose the isotropic exchange interaction which, depending on the sign of J_{nm}, tends to align the spins either parallel or antiparallel to one another.

The magnitude of the antisymmetric coupling constant may be estimated from the expression $|\underline{D}_{nm}| \approx (\Delta g/g) J_{nm}$. Consider a case with $\Delta g = 0.1$ and $J_{nm} = 100\ cm^{-1}$; we calculate $|\underline{D}_{nm}| \approx 5\ cm^{-1}$. This effect can be readily seen in EPR measurements, and in magnetic studies especially if J_{nm} is positive.

Let us examine the antisymmetric exchange interaction for the case of two exchange coupled S = 1/2 ions. The antisymmetric term is

$$\underline{D}_{12} \cdot [\underline{S}_1 \times \underline{S}_2] = \underline{D}_{12} \cdot \begin{vmatrix} \underline{i} & \underline{j} & \underline{k} \\ S_{1x} & S_{1y} & S_{1z} \\ S_{2x} & S_{2y} & S_{2z} \end{vmatrix}$$

$$= \underline{D}_x(S_{1y}S_{2z} - S_{2y}S_{1z}) + \underline{D}_y(S_{2x}S_{1z} - S_{1x}S_{2z}) + \underline{D}_z(S_{1x}S_{2y} - S_{2x}S_{1y})$$

If we take $\underline{D}_{12}$ along the Z axis, then

$$H_{antisymmetric} = \frac{iDz}{2} [S_{1-}S_{2+} - S_{1+}S_{2-}]$$

The Hamiltonian matrix for symmetric exchange, including an antisymmetric contribution, is

$$\begin{vmatrix} |\alpha\alpha\rangle & |\alpha\beta+\beta\alpha\rangle/\sqrt{2} & |\beta\beta\rangle & |\alpha\beta-\beta\alpha\rangle/\sqrt{2} \\ -1/2J-E & 0 & 0 & 0 \\ 0 & -1/2J-E & 0 & iD_z/2 \\ 0 & 0 & -1/2J-E & 0 \\ 0 & -iD_z/2 & 0 & 3/2J-E \end{vmatrix} = 0$$

This interaction mixes the $|S, M_s\rangle$ states $|1,0\rangle$ and $|0,0\rangle$ and results in a zero-field splitting of the triplet state. The roots of the determinantal equation are

$$E(|1,1\rangle, |1,-1\rangle) = -J/2$$

$$E(|1,0\rangle) = [J - J(4 - D_z^2/J^2)^{1/2}]/2$$

$$E(|0,0\rangle) = [J + J(4 + D_z^2/J^2)^{1/2}]/2$$

Exchange in Linear Chains. The exchange Hamiltonian for an infinite linear chain may be written as

$$H = -2J \sum_{i=1}^{\infty} \{\alpha \underline{S}_i{}^z S_{i+1}^z + \gamma(\underline{S}_i{}^x \underline{S}_{i+1}^x + S_i{}^y S_{i+1}^y)\} - g\beta H \sum_{i}^{\infty} \underline{H} \cdot \underline{S}_i \qquad (7)$$

For α, $\gamma = 1$, the isotropic Heisenberg case arises; while for $\alpha = 1$ and $\gamma = 0$, the anisotropic Ising case obtains; and for $\alpha = 0$, $\gamma = 1$, the relatively rare anisotropic X-Y case results. Fisher[7] has derived exact expressions for both the parallel and perpendicular magnetic susceptibilities for the anisotropic Ising case when $S = 1/2$. The parallel susceptibility is

$$\chi_{||} = \frac{Ng^2\beta^2}{4kT} \exp(2J/kT) \qquad (8)$$

while the perpendicular susceptibility is

$$\chi_{\perp} = \frac{Ng^2\beta^2}{8J} \{\tanh(J/kT) + (J/kT)\operatorname{sech}^2(J/kT)\} \qquad (9)$$

Bonner and Fisher carried out machine calculations on systems of chains containing from four to twelve spins, and extrapolated their results to the infinite-length chain.[11] The maximum in susceptibility is uniquely defined by the following relations:

$$\frac{kT_{max}}{|J|} \simeq 1.282 \; ; \qquad \frac{\chi_{max}|J|}{Ng^2\beta^2} \simeq 0.07346$$

Bonner and Fisher's numerical results can be reproduced by the expression[18a]

$$\chi_m = \frac{Ng^2\beta^2}{kT} \cdot \frac{A + Bx^{-1} + Cx^{-2}}{1 + Dx^{-1} + Ex^{-2} + Fx^{-3}} \qquad (10)$$

where $x = kT/|J|$, $A = 0.25$, $B = 0.14995$, $C = 0.30094$, $D = 1.9862$, $E = 0.68854$, and $F = 6.0626$. An alternate expression which gives comparable results has been given by Jotham.[18b] These expressions have the advantage of permitting the use of computer programs in the analysis of experimental data. This approach will surely be applied to other spin systems as the need arises.

Random Exchange in Linear Chains. The magnetic susceptibilities of mixed valence compounds which have one dimensional chain structures frequently reflect antiferromagnetic spin-spin coupling at moderate temperatures, but show an increase in susceptibility at low temperatures. In a regular chain of localized electrons, the susceptibility of a system of antiferromagnetically coupled metal ions with single localized electrons which can be described by the Heisenberg exchange Hamiltonian

(7) has a maximum value at $T_{max} = 1.282|J|/k$, and the susceptibility decreases to a finite value at 0°K. In periodically alternating chains the susceptibility decreases to zero at 0°K. Thus, neither of these models can explain the increase in susceptibility, and this feature is often attributed to the presence of small amounts of paramagnetic impurities which are trapped in the samples during the synthetic procedures. There is now good evidence from careful experimental work on highly purified samples that the low temperature increase in susceptibility is a intrinsic property of some of these compounds and that it arises from random exchange. This can be understood if one divides the entire system of spins into several noninteracting subsystems, of which some will have odd numbers of spins. These noninteracting residual spins will follow the Curie law, resulting in an increase in magnetic susceptibility at low temperatures.

Bulaevskii, et al[19] have derived very useful expressions for the thermodynamic properties of the system described above. Central to their derivation is the expression

$$\rho(\varepsilon) = Ak^{\alpha-1}\varepsilon^{-\alpha}$$

for the density of states, where A and α are parameters to be determined from experiment, and it is assumed that any dependence of ρ on T can be neglected at low temperatures, i.e. 0.1 to 10°K. The results from their derivation which are necessary for our discussion are equation (11) for magnetic susceptibility in the low field limit, i.e. where $g\mu_B H << kT$, and equation (12)

$$\chi(T,H\to 0) = 2(1-2^{1+\alpha})\zeta(-\alpha)\Gamma(1-\alpha)Ag^2\mu_B{}^2k^{-1}NT^{-\alpha} \qquad (11)$$

for the magnetization in the high field limit, i.e. where $g\mu_B H >> kT$.

$$M(0,H) = (1-\alpha)^{-1}g\mu_B NA(g\mu_B Hk^{-1})^{1-\alpha} \qquad (12)$$

In equation (11), $\zeta(x)$ is the Riemann zeta function and $\Gamma(x)$ is the gamma function. In practice, the adjustable parameters are determined by fitting these expressions to magnetic susceptibility and magnetization data.

Results which are close to these have been obtained by Theodorou and Cohen,[20] who used a disordered Hubbard model and investigated the effects of random antiferromagnetic exchange between spins. In their derivation the interaction parameter J followed a distribution function of the form $\rho(J) \propto J^{-\alpha}$, where $0 < \alpha < 1$. Theodorou and Cohen suggest that ε and $\rho(\varepsilon)$ of the Bulaevskii model are related to J and $\rho(J)$ of their work, thereby affording an explanation for the phenomenological density of states expression. Application of these ideas to exchange in

quinolinium $(TCNQ)_2$ by Azevedo and Clark[21] will be presented in Section on Representative Results.

Exchange in Two-Dimensional Sheets. The Hamiltonian appropriate for a two-dimensional magnetic system may be given by

$$H = -2J\sum_{i,j}(\underline{S}_{iz}\underline{S}_{jz} + \xi\underline{S}_{ix}\underline{S}_{jx} + \eta\underline{S}_{iy}\underline{S}_{jy}) \qquad (13)$$

$$-2J'\sum_{k,l}\underline{S}_n\cdot\underline{S}_l \ , \quad 0 < \xi, \eta < 1$$

where the S_{iw} (w = x, y, or z) are the components of the spin operator along the Cartesian coordinates, J and J' are the intra- and interlayer exchange constants, and the parameters ξ and η represent the anisotropy in the intralayer exchange. If the z-axis is taken as the easy axis of magnetization, then the anisotropy is Ising-like when $\xi = \eta < 1$ and when $\xi = 1$, $\eta < 1$ it is XY-like. The Heisenberg case arises when there is no anisotropy in the exchange. The various anisotropy parameters can be represented by effective fields by the use of the following molecular field equations for the parameters $D = 1 - \xi$ and $E = 1 - \eta$:[22,23]

$$H_{ex} = 2ZJ/g\mu_\beta$$

$$H_a^{in} = D\,H_{ex}$$

$$H_a^{out} = E\,H_{ex}$$

where H_{ex} is the effective exchange field arising from the intralayer exchange, and Z is the number of near neighbors within the layer. The contribution to the anisotropy arising from the anisotropic exchange interaction which favors parallel alignment within a layer can be estimated by the equations

$$H_{A,E} \approx 2Z\Delta JS/g\mu_\beta$$

$$\Delta J = J_{ac} - J_b \approx (\Delta g/\langle g\rangle)^2 J$$

where $\Delta g = g_{ac} - g_b$ and $\langle g\rangle = (2g_{ac} + g_b)/3$. In some cases it has been reported that the experimentally observed H_a^{out} is substantially smaller than the sum of the theoretical components which are expected to be most important.[24,25] This immediately suggests that there must be an additional contribution to the anisotropy arising from exchange interactions either within the layer or between layers. One such additional term which does exist for these systems is antisymmetric (Dzialoshinki - Moriya) exchange which was discussed above.

Exchange in Three Dimensional Polymers. Exchange interactions between paramagnetic ions in three dimensional arrays may lead to ferromagnetism, ferrimagnetism, or antiferromagnetism. In ferromagnetic substances the magnetic dipoles are all oriented in the same direction, while in ferrimagnetic or antiferromagnetic substances there are two or more interpenetrating lattices of magnetic dipoles which generally are oriented in different directions. The description of magnetic properties of three dimensional mixed-valence compounds usually requires two or more sublattices since the paramagnetic ions are nonequivalent. Strictly speaking, all of these compounds should be ferrimagnets, but if all sublattices have their magnetic dipoles oriented in the same direction, then the properties would not be different from those of ferromagnets. For the purposes of this discussion the theory of ferrimagnetism developed by Néel will be required.[26]

Consider a situation in which there are *A* and *B* sites forming two sublattices. The molecular field experienced by an ion on site *A* is $\underline{H} = (2zJ_{ab}/N_b g_a g_b \mu_B^2)\underline{M}_b$, where z is the number of nearest neighbors and J_{ab} is the coupling constant. The multiplier of the magnetic moment of the *B* sublattice is the molecular field coefficient γ_{ab}. Interactions between the paramagnetic ions lead to the following molecular fields: $\underline{H}_{aa} = \gamma_{aa}\underline{M}_a$; $\underline{H}_{ab} = \gamma_{ab}\underline{M}_b$; $\underline{H}_{bb} = \gamma_{bb}\underline{M}_b$; $\underline{H}_{ba} = \gamma_{ba}\underline{M}_a$.

The total fields experienced by *A* and *B* atoms are given by

$$\underline{H}_a = \underline{H}_o + \gamma_{aa}\underline{M}_a \pm \gamma_{ab}\underline{M}_b$$

and

$$\underline{H}_b = \underline{H}_o + \gamma_{bb}\underline{M}_b \pm \delta_{ab}\underline{M}_a .$$

where $\underline{H}_o$ is the applied field. Following Smart,[15] let *N* be the total number of paramagnetic ions, λ be the fraction on *A* sites, μ be the fraction on *B* sites, and name the sites such that $\lambda \leq \mu$. Also, let $\alpha = \gamma_{aa}/\gamma_{ab}$, $\beta = \gamma_{bb}/\gamma_{ab}$, $\sigma_a = \underline{M}_a/\lambda N g \mu_B S$, and $\sigma_b = \underline{M}_b/\mu N g \mu_B S$. The molecular fields become

$$\underline{H}_a = \underline{H}_o + Ng\mu_B S\gamma_{ab}(\lambda\alpha\underline{\sigma}_a \pm \mu\underline{\sigma}_b)$$

$$\underline{H}_b = \underline{H}_o + Ng\mu_B S\gamma_{ab}(\pm \lambda\underline{\sigma}_a + \mu\underline{\sigma}_b)$$

Two cases can be identified, one of these has $J_{ab} > 0$ and the other has $J_{ab} < 0$. For the case with a positive *A*-*B* interaction the high temperature susceptibility becomes

$$\chi = \frac{C[T + \lambda\mu C\gamma_{ab}(2 - \alpha - \beta)]}{T^2 - C\gamma_{ab}(\lambda\alpha + \mu\beta) + \lambda\mu C^2\gamma_{ab}^2(\alpha\beta - 1)} \qquad (14)$$

Néel recognized that the $\chi^{-1} \cdot T$ curve is a hyperbola of the form

$$\chi^{-1} = \frac{T-\theta}{C} - \frac{\zeta}{T-\theta'}, \tag{15}$$

with $\theta = C\gamma_{ab}\lambda\mu(2 + \lambda\alpha/\mu + \mu\beta/\lambda)$

$\theta' = -C\gamma_{ab}\lambda\mu(2 - \alpha - \beta)$

$\zeta = C\gamma_{ab}^{2}\lambda\mu(\lambda\{1 - \alpha\} - \mu\{1 - \beta\})^{2}$

The hyperbola may be alternately expressed as

$$\chi^{-1} = \frac{(T - T_c)(T - T_c')}{C(T - \theta')} \tag{16}$$

The hyperbola is sketched in Figure 1, and the constants are designated there. In order to treat the case in which $J_{ab} < 0$, the signs of γ_{ab}, α, and β are taken to be negative, and it is possible to obtain the parameters in the theory by fitting the expression for susceptibility to experimental data. Many examples are given in the recent treatise by Craik.[27]

DATA ANALYSIS

While measurements of magnetic properties at one temperature (say, room temperature) or over a limited temperature range yield data which are more valuable than none at all, it must be emphasized that measurements over wide ranges of temperatures and fields are usually essential for a detailed description of electronic structure and bonding.

The first step in the analysis of the data is to plot the molar magnetic susceptibility, χ_m, which has been corrected for the diamagnetism of the constituents, versus T^{-1}. If a straight line which passes through the origin is obtained, then Curie law behavior, $\chi_m = C/T$, is followed. From the Curie constant, one can calculate μ_{eff} using the expression $\mu_{eff} = 2.828\ (\chi \cdot T)^{1/2}$ and use the Bohr magneton number along with complementary data to solve the problem at hand. If a straight line which intercepts the positive χ-axis at $T^{-1} = 0$ is obtained, it is possible that temperature independent paramagnetism is present, or that the diamagnetic correction has been overestimated. If the straight line intercepts the negative χ-axis at $T^{-1} = 0$, it is likely that the diamagnetic correction has been underestimated.

For mixed-valence, it more likely that a Curie-Weiss law will be required to fit the data, and that this law will hold only over a limited temperature range. The Curie-Weiss law was

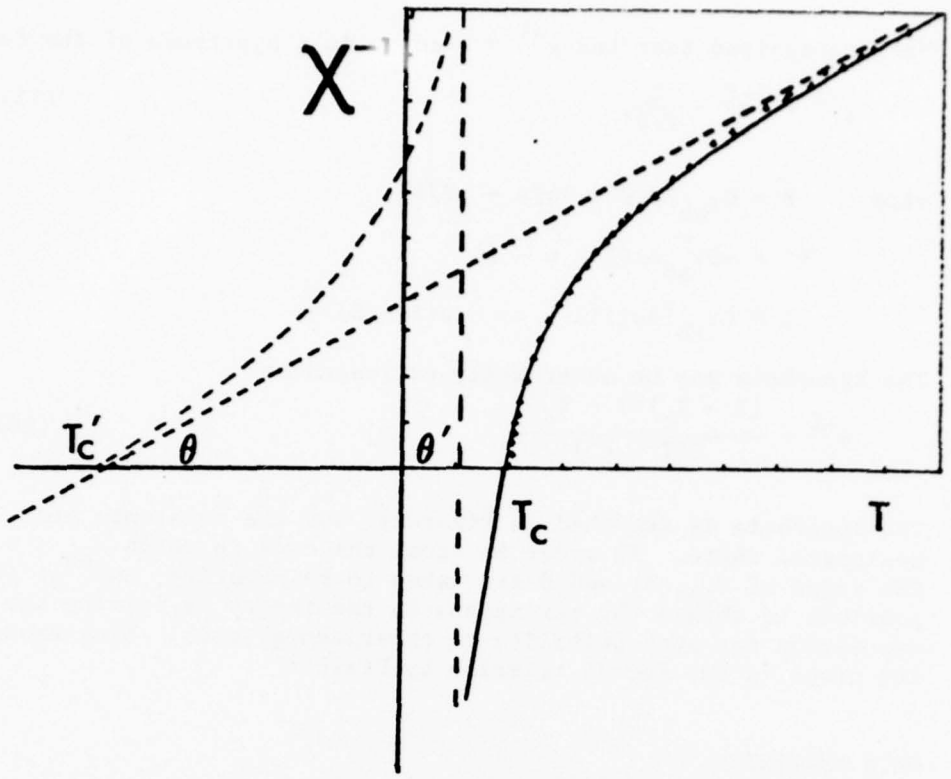

Figure 1. A sketch of the Néel hyperbola with the parameters indicated.

derived above. It is usually instructive to plot $\chi \cdot T$ versus T. Curie law behavior holds if a straight line parallel to the T axis is obtained. For orbitally nondegenerate systems deviations from straight line behavior toward larger $\chi \cdot T$ values indicate ferromagnetic interactions, while deviations toward smaller $\chi \cdot T$ values indicate antiferromagnetic behavior.

A serious complication in the interpretation of magnetic data may arise if ferromagnetic impurities are present even in small quantities. In favorable cases it is possible to account for such impurities by making measurements as a function of magnetic field strength. Generally, for a saturated ferromagnet the force exerted in a Faraday measurement, for example, is proportional to $d\underline{H}/dz$, while that exerted on a paramagnetic substance is proportional to $\underline{H}(d\underline{H}/dz)$. The intrinsic susceptibility of the sample χ_i is given by the measured susceptibility χ_H minus the quantity $C\sigma_s/\underline{H}$ where C is the concentration of the ferromagnetic impurity and σ_s is the saturation magnetization. If a plot of χ_H versus 1/H yields a straight line the correction can be made readily.

Units for Magnetic Properties. There are two systems of units commonly used in publications dealing with magnetic properties. These are the cgs-emu system and the International System of Units (SI). Quickenden and Marshall[28] and Mulay[29] have presented definitions of the quantities that are encountered and have discussed the relationship of these quantities in the two systems. A very convenient table of conversion factors has been compiled by Bennett, Page, and Swartzendruber[30] and is reproduced here in Table I.

REPRESENTATIVE RESULTS

Since a complete survey of the magnetic properties of mixed valence systems is outside the scope of this chapter, results from representative studies only are summarized here. The discussion in this section is intended to illustrate the scope and the complexity of the field and hopefully will serve as a stimulus for additional research; some specific problem areas are identified.

Clusters

Di-μ-oxobis[bis(2,2'-bipyridine)manganese(III,IV)]. This unusual complex was first prepared by Nyholm and Turco,[31] and the structure was determined by Palenik and coworkers.[32] As the bond distances in Figure 2 show, the two manganese ions are distinctly different, and the shorter bond distances from the donor atoms to Mn(2) indicates that Mn(2) is the Mn(IV) ion. In addition, the lengthening of the quasi axial bonds of Mn(1) is comparable to the lengthening of such bonds in Mn(III) complexes, and it is reasonable to assign the oxidation state +3 to Mn(1).

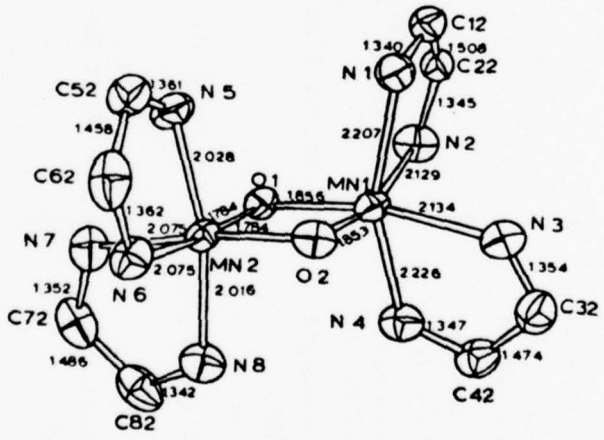

Figure 2. The structure of di-μ-oxobis[bis(2,2'-bipyridine)-manganese(III,IV)]. Reprinted with permission from Reference 32.

Table I. *Conversion Factors for Magnetic Quantities.*

Multiply the Number for		By	To Obtain the Number for	
Gaussian Quantity	Unit		SI Quantity	Unit
flux density, B	G	10^{-4}	flux density, B	T($\equiv Wb/m^2$ $\equiv Vs/m^2$)
magnetic field strength, H	Oe	$10^3/4\pi$	magnetic field strength, H	A/m
volume susceptibility, χ	emu/cm^3 (dimensionless)	4π	rationalized volume susceptibility, κ	dimensionless
mass susceptibility, $\chi\rho$	$emu/g(\equiv cm^3/g)$	$4\pi \cdot 10^{-3}$	rationalized mass susceptibility, κ_ρ	m^3/kg
molar susceptibility, χ_{mole}	$emu/mol(\equiv cm^3/mol)$	$4\pi \cdot 10^{-6}$	rationalized molar susceptibility, κ_{mole}	m^3/mol
magnetization, M	G or Oe	10^3 $4\pi \cdot 10^{-4}$	magnetization, M magnetic polarization, J	A/m T
magnetization, $4\pi M$	G or Oe	$10^3/4\pi$ 10^{-4}	magnetization, M magnetic polarization, J	A/m T
magnetization, M	μ_B/atom or μ_B/form. unit, etc.	1	magnetization, M	μ_B/atom or μ_B/form, unit, etc.
magnetic moment of a dipole, m	erg/C	10^{-3}	magnetic moment of a dipole, m	$J/T(\equiv Am^2)$
demagnetizing factor, N	dimensionless	$1/4\pi$	rationalized demagnetizing factor, N	dimensionless

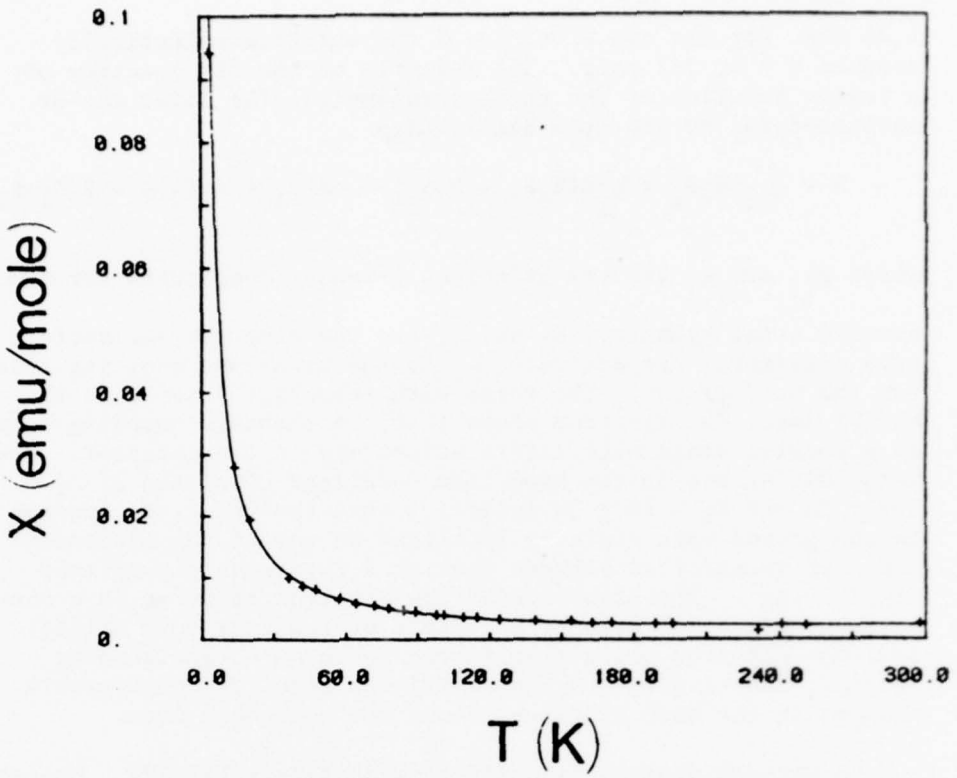

Figure 3. The magnetic susceptibility data for di-μ-oxobis-[bis(2,2'-bipyridine)manganese (III,IV)]. The experimental data are given by +, and the solid line is the best fit to the expression for an exchange coupled S = 2, 3/2 pair.

Cooper, Calvin, and coworkers[33,34] have recently carried out extensive studies including spectroscopic, magnetic, and electrochemical measurements on the di-μ-oxo-2,2'-bipyridine complex as well as the 1,10-phenanthroline analogue. Their magnetic susceptibility data are shown in Figure 3, where the solid line is the best fit to the data of equation 17 for an exchange coupled S = 2, 3/2 pair using J = -150 cm^{-1}, the EPR

$$\chi_m = \frac{Ng^2\mu_B^2}{4kT} \cdot \frac{84\exp(6J/kT) + 35\exp(-J/kT) + 10\exp(-6J/kT}{4\exp(6J/kT) + 3\exp(-J/kT) + 2\exp(-6J/kT)} \cdots$$

$$\cdots \frac{+ \exp(-9J/kT)}{+\exp(-9J/kT)} + N\alpha \qquad (17)$$

<g> value of 2.0, and an assumed value of 120 x 10^{-6} cgs for the temperature independent paramagnetism, Nα. The 1,10-phenanthroline compound has J = -134 cm^{-1}; Cooper and Calvin[33] attribute the small difference in J values to a more favorable exchange interaction geometry for the more flexible 2,2'-bipyridine ligand. The compounds exhibit moments of 1.75 B.M. and 1.74 B.M. at the low temperature limit of the experimental measurements consistent with the expected spin-only moment of

1.73 B.M. for the odd electron of the antiferromagnetically coupled S = 2, 3/2 pair. The features of the EPR spectrum of a frozen solution of the phenanthroline(III,IV) dimer may be accounted for by the spin Hamiltonian

$$H = g_{||}\beta H_z S_z + g_{\perp}\beta(H_x S_x + H_y S_y) + (A_1 I_1 + A_2 I_2)S - 2JS_1 \cdot S_2$$

where $g_{||}$ and $g_{\perp}$ are the principal g-tensor components for the assumed axial symmetry, S_1 and I_1 are the electron and nuclear spin operators, respectively, A_1 is the hyperfine coupling tensor for the Mn(III) ion. The terms with subscript 2 refer to the Mn(IV) ion. The spectrum shows that the exchange coupling results in a doublet state with little anisotropy in the g-tensor. The large difference in the hyperfine couplings constants of A_1 = 167 $\pm$ 3G and A_2 = 79 $\pm$ 3G indicates that the unpaired electron in the ground spin state is localized on one of the manganese ions, or transferred between them at a rate much slower than $|A_1| - |A_2|$. The slow rate of the electron transfer is a consequence of the electronic structure of the high spin Mn(III) ion; the electron being transferred is in an e_g antibonding orbital, and transfer to the Mn(IV) ion requires considerable changes in the bond distances about the manganese ions.

μ-Oxo-μ-hydroxobis[(Schiff base)manganese(III,IV). Magnetic susceptibility studies on a series of bimetallic manganese compounds with the Schiff bases

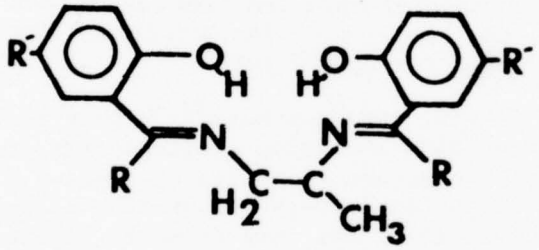

R = H (≡Sol), R = CH_3 (≡Acet)

revealed that the compounds should be formulated as mixed oxidation state dimers of manganese(III) and manganese(IV), i.e. as $[Mn_2(SB)_2(OH)O]\cdot nH_2O$.[35] Magnetic moments of 10% TMS-$CHCl_3$ solutions of the complexes (~0.002 M) were determined by the NMR method at ambient temperature with a 250-MHz spectrometer. The compound $[Mn_2(BuSalpn)_2(OH)O]\cdot H_2O$ exhibited a magnetic moment of 2.30 BM while $[Mn_2(BuAcetpn)_2(OH)O]\cdot 2H_2O$ has a moment of 2.64 BM. These compounds, which may be examples of Class II, have a new band in their visible absorption spectrum at ~21-22,000 cm^{-1}. This absorption band, which is responsible for the cherry

red color of the compounds, has been assigned as the intervalence band. If this assignment is correct then the degree of interaction must be rather small since the frequency of the transition occurs in the denominator for α.

Biferrocene(II,III) Picrate. Kaufman and Cowan [36,37] recognized that the ligands usually employed in mixed valence chemistry, up to advent of their work, were not readily susceptible to structural variations and conjectured that organometallic compounds would be very good systems for systematic work. They selected metallocenes as the first candidates for their studies for the following reasons: (1) Strong interactions between mixed valence sites are to be expected when the orbitals on these centers have the same symmetry and are close enough for appreciable overlap, and metallocenes have these properties. (2) Delocalization is enhanced when the ligand field strengths of the mixed valence ions is similar. (3) Available crystallographic data on ferrocene and its salts had revealed that the formal oxidation state of the iron atom has little effect on the interatomic distances, and consequently the reorganization energy would not be expected to be very large. (4) Metallocenes exhibit strong interactions between the metal orbitals and the unsaturated π system of the cyclopentadienyl rings, and mixed valence delocalization could possibly be transmitted by metal-ligand orbital overlap. The spectroscopic and electrical conductivity measurements of Kaufman and Cowan on biferrocene(II,III) picrate (19) demonstrated that electron transfer in this system is quite facile.

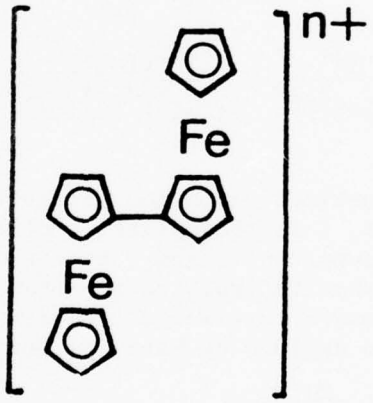

The ultraviolet to near infrared spectrum of a solution of biferrocene(II,III) picrate in acetonitrile exhibited bands at 220 and 295 nm which were assigned to the substituted ferrocene portion of the molecule, a broad band at 550-600 nm which was assigned to ferrocenium portion of the molecule, and a new, broad band centered at 1900 nm (ε 551), which was assigned to

the electron-transfer transition. A rate of electron transfer of 1.3×10^{10} sec^{-1} was calculated from the energy of this band on the basis of Hush's theory.[38] The interaction parameter α was also calculated using equation (20)

$$\alpha^2 = \frac{4.5 \times 10^{-4}\, \varepsilon_{(max)} \Delta(1/2)}{(\bar{\nu})(r^2)} \qquad (20)$$

where $\varepsilon_{(max)}$ is the molar absorptivity at the band maximum, $\Delta(1/2)$ is the band half-width in wavenumbers, $\bar{\nu}$ is the energy of the intervalence transfer band in wavenumbers, and r is the distance between donor and acceptor sites in Angstroms. This equation, which is valid only for cases in which there are weak interactions, yields the value 0.095 for α, which signifies a weak interaction between the mixed valence sites of this Class II system.

The magnetic properties of the picrate and tetrafluoroborate salts of biferrocene(II,III) were measured over the range 2-300 K.[39] Expressions for the temperature dependence of the magnetic susceptibility had been derived earlier[40] for the set of two Kramer's doublets of the $^2E_{2g}$ ground state of the ferrocenium ion and these were used for the analysis of the data. The equations are

$$\chi_{||}(E'') = \frac{N\beta^2}{kT}\left[\left(1 + \frac{2k'(1-\zeta^2)}{(1+\zeta^2)}\right)^2 + \frac{16\zeta^2 k'^2 (kT)}{(\zeta^2+\delta^2)^{1/2}(1+\zeta^2)^2}\right] \qquad (21a)$$

$$\chi_{\perp}(E'') = \frac{N\beta^2}{kT}\left[\frac{4\zeta^2}{(1+\zeta^2)^2} + \frac{2kT(1-\zeta^2)^2}{(1+\zeta^2)^2(\xi^2+\delta)^{1/2}}\right] \qquad (21b)$$

where k' is the orbital reduction parameter, ξ is the spin-orbit coupling constant, δ is the splitting of the energy levels due to low symmetry components, and ζ is the wave function mixing parameter which results from the departure from axial symmetry. These constants may be estimated from EPR results using the g-value expressions derived by Maki and Berry:[41]

$$\begin{aligned} g_{\perp} &= 4\zeta/(1+\zeta^2) \\ g_{||} &= 2 + 4k'(1+\zeta^2)/(1+\zeta^2) \\ |\zeta| &= x/[1 + (1+x^2)]^{1/2} \\ |x| &= \delta/k'\xi \end{aligned} \qquad (22)$$

Table II. *Magnetic Parameters for Ferrocenium Compounds.*

Compound	T, °K	$g_{\|\|}$	$g_{\perp}$	μ_{eff} [a]	μ_{eff} [b]	$\|\zeta\|$	k'	$\|\delta\|$ [c]	$\|\delta\|$ [d]
Biferrocene(3,3)$(BF_4)_2$ [e]	298	3.2	1.91	3.42	3.53	0.74	1.0	660	750
Biferrocene(2,3) picrate	77	$\langle g \rangle$ =	2.42	2.10	2.21	--	-	985	1000
Biferrocene(2,3) picrate	77	3.52	1.85	2.18	2.23	0.67	1.0	---	--
$(C_6H_5C_5H_4)_2Fe^+$ [e,f]	20	3.62	1.75	--	--	0.58	0.82	580	--
$(C_5H_5)_2Fe^+$ [e,f]	20	4.35	1.26	--	--	0.36	0.76	270	--

[a] Determined from $\mu = [(g_{||}^2/3 + 2g_{\perp}^2/3)S(S+1)]^{1/2}$.

[b] From direct measurement.

[c] Units of cm^{-1} per ferrocenium unit.

[d] Best fit from susceptibility.

[e] Frozen solution.

[f] Sohn, Y.S.; Hendrickson, D.N.; Gray, H.B. J. Am. Chem. Soc. 1970, 92, 3233.

ferrocenium salts.

The Mössbauer spectrum of BFD(II,III) salts exhibit only two lines, and this observation leads to the conclusion that the two iron atoms are identical on the Mössbauer time scale. There are, of course, two possible explanations for this observation. There could be rapid electron transfer of a class II system or delocalization in a class III system. This latter description is further supported by ESCA and EPR data. BFD(II,III) picrate and tetrafluoroborate have the same g-values in the solid and in glasses, where $g_1 = 1.87$, $g_2 = 2.00$, and $g_3 = 2.27$. The effective magnetic moment calculated from $\mu_{eff} = [1/3(g_1^2 + g_2^2 + g_3^2)S(S+1)]^{1/2}$ is 1.78 μ_B, a value which is in good agreement with the magnetic susceptibility result.

Although there is a broad, intense band in the near infrared at 1550 nm, with a second band at 1140 nm, from which a delocalization of 3% may be calculated, the magnetic properties, EPR, ESCA, and Mössbauer data rule out the assignment of this band to intervalence transfer.

Principally through the work of Davidson, Smart and coworkers,[48,49] additional examples of bisfulvalene-dimetal compounds and mono- and dioxidized salts have been prepared. Compounds of iron (see above), nickel, and cobalt are known. For these, all BFD-M(II,II) compounds are diamagnetic, all BFD-M(II, III) compounds are paramagnetic with $\mu_{eff} \sim 1.7$ B.M. and the moments are temperature independent, and all BFD-M(III,III) compounds are diamagnetic. $[BFD\text{-}Co]^{z+}$ (z = 0, 1) exhibit bands in the electronic absorption spectrum at 980 nm with $\varepsilon = 1150$ for z = 0 and $\varepsilon = 7000$ for z = +1. The electron spectrum of $[BFD\text{-}Ni]^{z+}$ (z = 0, 1, 2) also exhibit similar bands. Smart and Pinsky[49] state that these bands "are not intervalence transfer transitions associated with electron transfer from one localized metal center to another".

The compound 3-vinylbisfulvalenediiron(II,II) has been prepared and homopolymerized in benzene using azobis(isobutyronitrile) initiation. The polymer was oxidized with TCNQ to yield mixed valence polymers with a range of stoichiometries as measured by the ratio $BFD^+/(BFD^+ + BFD)$.[50] The dark conductivity of the sample in which 71% of the bisfulvalenediiron units were monooxidized was 6-9 x 10^{-3} ohm^{-1} cm^{-1}. Magnetic data are not available for these substances.

Oxo-bridged Mixed Valence Diiron(III,IV) Complexes. Wollman and Hendrickson[51] have measured the mixed valence compounds $[Fe_2(TPP)_2O]X$ (TPP = tetraphenylporphinates, $X \equiv PF_6^-$, BF_4^-) and $[Fe_2(salen)_2O]X$ [salen = N,N'-ethylenebis(salicylideniminato), $X^- = PF_6^-$, ClO_4^-, BF_4^-, I_3^-], and have analyzed the data in terms

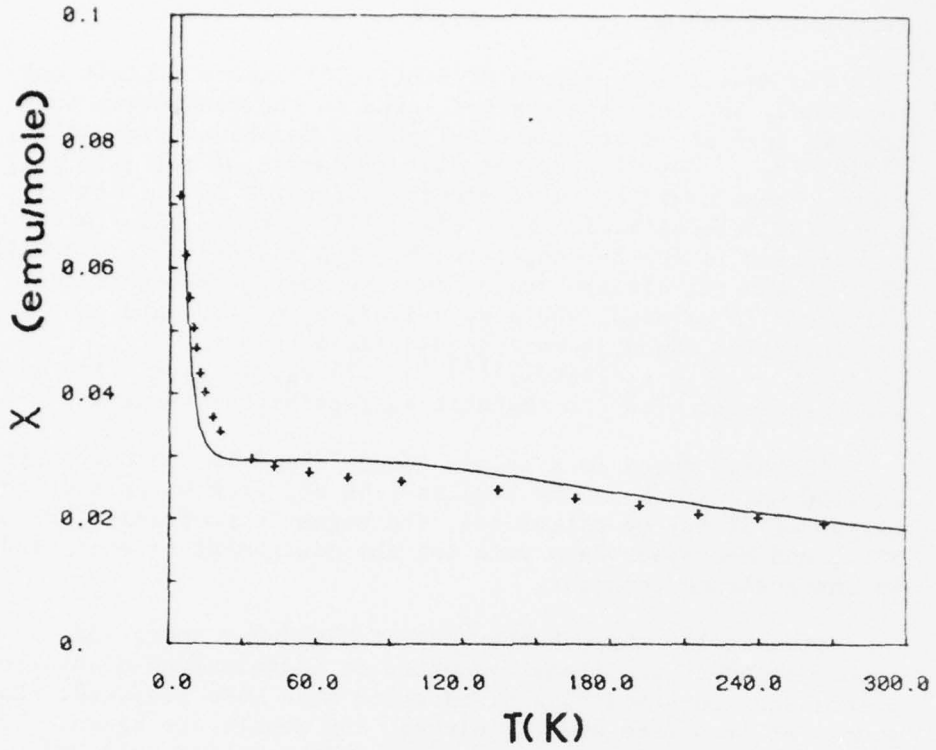

Figure 4. Magnetic susceptibility data for μ-oxo-bis[salen Fe-(III,IV)].

of isotropic exchange of an S = 5/2, 2 pair with a small zero field splitting for the salen compounds and a large zero field splitting for the porphyrin complexes. Unfortunately, as shown in Figure 4 the fit of the Van Vleck equation including a mean field interdimer exchange term to the data for $[Fe_2(salen)_2O](PF_6)$ is not especially good, but the low temperature limiting moment of 1.2 μ_B is in good agreement with the expectation of one unpaired electron per pair of iron ions. The magnetic parameters for these compounds are collected in Table III, where the range of

Table III. *Magnetic Parameters for Oxo-bridged Iron(III,IV) Dimers*

Compound	J,cm^{-1}	Z'J',K	|D|,cm^{-1}	$g_{\|\|}$	$g_{\perp}$
$[Fe_2(salen)_2O]PF_6$	-11.6	-0.05			
$[Fe_2(salen)_2O]ClO_4$	-17.6	-1.6			
$[Fe_2(salen)_2O]BF_4$	-8.7	-2.3			
$[Fe_2(salen)_2O]I_3 \cdot CHCl_3$	-7.5	-5.9			
$[Fe_2(TPP)_2O]PF_6$	-119	...	11.7	2.34	5.47
$[Fe_2(TPP)_2O]BF_4$	-82.5	...	19.9	3.11	4.80

exchange coupling constants, mean field intercluster correction terms, zero-field splitting energies, and g-values may be seen to vary over a very wide range.

The Mössbauer spectra of $[(Fe_2salen_2)O]X$ and $[(Fe_2TPP_2)O]X$ were recorded at 77° and 4.2°K, and consisted of a single quadrupole-split doublet in each case. Thus, the mixed valence iron compounds have identical iron ions on the Mössbauer time scale. This means that the rate of electron transfer is faster than $\sim 10^7 sec^{-1}$ in both series of compounds. The EPR spectra of the *salen* compounds exhibit one line whose line-width is slightly temperature dependent, a property to be expected if the rate of electron transfer is comparable to the EPR time scale, about $10^{10} sec^{-1}$. The EPR spectrum of $[Fe_2TPP_2O]PF_6$ was reported to be highly anisotropic, a result which is at variance with earlier observations[52] on $[Fe_2TPP_2O](ClO_4)$. Furthermore, no EPR signal was seen for the tetraflucroborate salt, and no absorption bands were observed in the near-IR region of the spectra of any of the compounds. It is clear that the oxy-bridged mixed valence iron compounds are not understood very well and that more careful work is needed.

A Nitrido-Bridged Iron Complex. The only example of a nitrido-bridged complex of a first-transition series element was prepared by Summerville and Cohen.[53] The thermal decomposition of [Fe(III)(TPP)N_3], where TPP is tetraphenylporphine, in the absence of oxygen yields [{Fe(TPP)}$_2$N] plus nitrogen gas. The Mössbauer spectra show that the two iron atoms are equivalent, and the Mössbauer parameters are consistent with a higher oxidation state for the iron atoms than those in [{Fe(TPP)}$_2$O].

A magnetic susceptibility study on [{Fe(TPP)}$_2$N] yielded a temperature independent moment of 2.04 μ_B per dimer. Based on a comparison of the Mössbauer quadrupole splitting constant of 1.08 mm sec^{-1} for the nitrido-bridged complex with the usual values of 1.25 to 2.11 mm sec^{-1} for low spin iron(III) hemichromes, Cohen concluded that the iron ions were high-spin and strongly coupled.[1] The data do not permit a classification in the Robin and Day[2] scheme of this fractional oxidation state complex.

[Ni_2(1,8-naphthyridine)$_4X_2$]Y. A series of complexes of this general formula with X = halide, NCS^-, NO_3^- and Y = PF_6^- or $B(C_6H_5)_4^-$ may be prepared by mixing boiling butan-1-ol solutions of the nickel(II) salt, the ligand, and sodium tetraphenylborate.[54a] On further boiling black crystals may be obtained. In the case of the hexafluorophosphate salts, it is necessary to add sodium tetrahydroborate in order to get the desired product. X-ray structural results for [Ni_2(napy)$_4Br_2$]$B(C_6H_5)_4$ reveal that the nickel ions of formal oxidation state +1.5 have identical coordination environments which are square pyramidal. The base of the pyramid is formed by four nitrogen atoms from four different ligand atoms and the apex of the pyramid is occupied by a bromide ion. These two equivalent pyramids are held together by the four bridging naphthyridine ligands with a very short nickel-nickel separation of 2.415(4) Å. The bases of the two tetragonal pyramids are staggered with a twist angle of about 25° along the Br-Ni-Ni-Br axis, which is nearly linear.

The magnetic moments of these complexes are in the range 4.19-4.33 μ_B per formula unit, values which are in agreement with the presence of three unpaired electrons. A variable temper- Weiss constant of -3 K. More extensive magnetic measurements would be of much interest since EPR studies show that the molecule has a quartet ground state as a result of a large ferromagnetic intracluster coupling.[54b] An analogous copper(I)-copper(II) complex has also been characterized.[54c]

Macrocyclic Mixed Valence Copper(I)-Copper(II) Complex. Condensation of 5-methyl-2-hydroxyisophthalaldehyde with 1,3-diaminopropane in the presence of copper(II) perchlorate yields the complex[55]

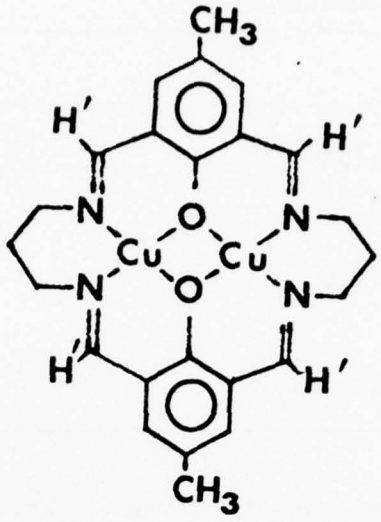

(24)

Electrolysis of an acetonitrile solution at -0.7 V followed by an addition of ether yields a nearly black solid with the formula $[Cu(I)Cu(II)L](ClO_4)$. A new solvent dependent band in the electronic spectrum of the mixed valence complex at about 900-1200 nm was assigned to an intervalence transfer transition. At room temperature, the EPR spectrum exhibits seven lines, while in frozen solutions only four lines are present.[56] These observations suggest that the odd electron interacts with both copper ions by a rapid transfer process at room temperature but is localized on a single copper ion at low temperature. If the primed hydrogen atoms in (24) above are replaced by methyl groups, a four line spectrum is observed even at room temperature.[57] The steric requirements of the methyl groups probably affect the conformation of the macrocycle and inhibit thermal electron transfer on the EPR time scale.

The room temperature magnetic moments of a number of related complexes are given in Table IV. The data show that the copper(II) ions in the complex $[Cu(II)Cu(II)L](ClO_4)_2 \cdot 2H_2O$ are antiferromagnetically exchange coupled. An explanation of the significant difference between the moments of $[Cu(II)Cu(I)L](ClO_4)$ and the carbonyl adduct will require more extensive magnetic data.

μ-Oxo-Bridged Ruthenium Complexes. Meyer and coworkers[58] have studied a number of mixed valence oxo-bridged ruthenium complexes, and based on chemical, electrochemical, ESCA, magnetic, and spectroscopic data have concluded that complexes typified by the salt $[(bipy)_2ClRuORuCl(bipy)_2](PF_6)_3$ belong to class III. As usual in this research, the approach adopted was a comparison

Table IV. *Magnetic Moments at 25°C*

Compound	μ_{eff}, μ_B
$[Cu^{II}Cu^{II}L](ClO_4)_2 \cdot 2H_2O$	0.60 ± 0.04
$[Cu^{II}Cu^{I}L](ClO_4)$	1.81 ± 0.04
$[Cu^{II}Cu^{I}L(CO)](ClO_4)$	1.94 ± 0.04
$[Cu^{I}Cu^{I}L]$	0.19 ± 0.25
$[Zn^{II}Zn^{II}L](ClO_4)_2 \cdot 2H_2O$	0.00 ± 0.25

of properties of complexes in a range of oxidation states. The structure of the like valence compound $[(bipy)_2(NO_2)Ru\text{-}O\text{-}Ru(NO)_2\text{-}(bipy)_2](ClO_4)_2 \cdot 2H_2O$ has been reported,[59] and the oxo-bridge formulation confirmed.

The (III,III) compounds are paramagnetic at room temperature with moments on the order of 1.8 μ_B per ruthenium ion. The magnetic moments are consistent with the ruthenium(III) ions being in the low-spin $4d^5$ electronic configuration. Variable temperature magnetic measurements were made on $[(bipy)_2(NO_2)Ru\text{-}O\text{-}Ru(NO_2)(bipy)_2](PF_6)_2$ and $[(phen)_2(NO_2)Ru\text{-}O\text{-}Ru(NO_2)(bipy)_2](ClO_4)_2$. The magnetic susceptibility of the 2,2'-bipyridine complex maximizes at about 155 K, while that of the 1,10-phenanthroline salt shows the same property at about 110 K. The magnetic susceptibility data may be fit very accurately with the Van Vleck equation for systems consisting of a singlet ground state and a low lying triplet state. The magnetic parameters which resulted from a least squares fitting of the Van Vleck equation to the data are

	2,2'-bipyridine salt	1,10-phenanthroline salt
$2J$, cm^{-1}	-173	-119
$\langle g \rangle$	2.48	2.29

The magnetic data can be interpreted in two ways. One interpretation would assume strong coupling in a delocalized system, while the second approach would invoke moderate spin-paired interaction between two low-spin ruthenium(III) ions. In view of the short ruthenium-oxygen bonds which should result in strong spin-spin coupling and much larger $|2J|$ values, and the chemical and spectroscopic properties of the complexes it is reasonable to conclude that the system is delocalized. The following

qualitative molecular orbital diagram based on the model developed by Dunitz and Orgel[60] should apply:

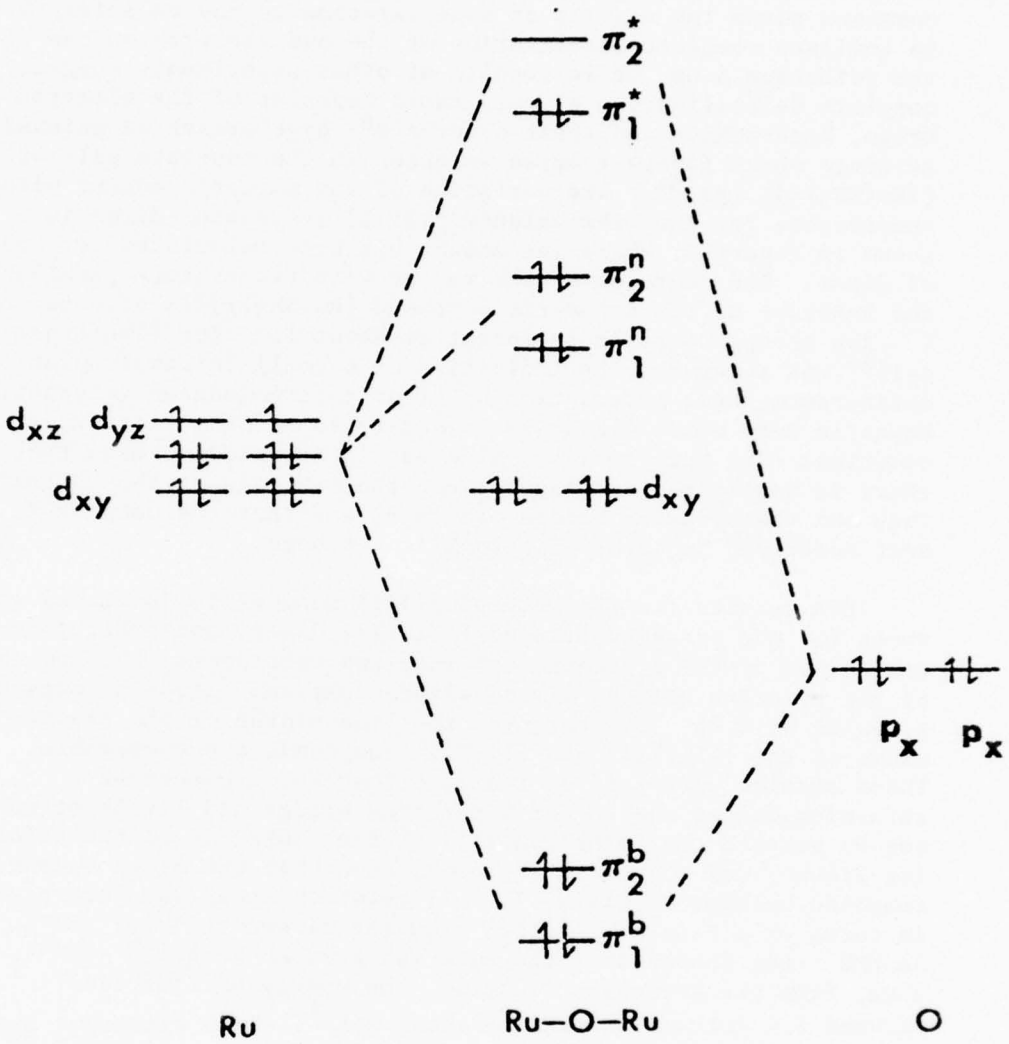

If this scheme applies, then 2J is a measure of the energy difference between a singlet state of the type $^1(\pi_1{}^*{}^2)$ and the triplet state $^3(\pi_1{}^*\pi_2{}^*)$, with the singlet state $^1(\pi_1{}^*\pi_2{}^*)$ being at higher energy than $^3(\pi_1{}^*\pi_2{}^*)$ because of Hund's rules. The low energy intense bands in the electronic spectra can be assigned to the transitions $\pi^b \rightarrow \pi^*$. Formation of the mixed valence complexes, such as $[(bipy)_2ClRu\text{-}O\text{-}RuCl(bipy)_2]^+$ would involve addition of an electron to $\pi_2{}^*$, and this process should destabilize the Ru-O-Ru linkage. The chemical instability of salts of $[(bipy)_2\text{-}ClRu\text{-}O\text{-}RuCl(bipy)_2]^+$ are consistent with this explanation.

μ-Pyrazine-bis[pentaammineruthenium(II,III)] Ion. The mixed valence ion $[\{Ru(NH_3)_5\}_2pyr]^{5+}$ has been the subject of many discussions since the results of some experiments may be interpreted to indicate complete localization of the odd electron on one of the ruthenium ions, while results of other experiments suggest complete delocalization or very rapid transfer of the electron. Drago, Hendrickson and their coworkers[61] have presented extensive evidence which favors trapped valences in the tosylate salt of $[\{Ru(NH_3)_5\}_2\ pyr]^{5+}$. The variation of the magnetic moment with temperature for the like valence [III,III]-pyrazine dimer is shown in Figure 5, where the moment has been calculated per mole of dimer. The decrease of the moment with temperature parallels the behavior of the monomeric compound $[Ru(NH_3)_6]Cl_3$ down to 15 K. The abrupt decrease in moment at about 15 K for $[\{Ru(NH_3)_5\}_2$-$pyr]^{6+}$ was thought to be indicative of a small intramolecular antiferromagnetic interaction or of an intermolecular interaction. Magnetic data below 4.2 K are necessary to resolve this important question. The very small J value was interpreted to mean that there is negligible overlap between the orbitals of the ruthenium ions and the pyrazine bridge orbitals, and that the complex is best described in terms of a localized scheme.

EPR results for the ruthenium(III) monomer is identical with those for the pyrazine bridged [III,III] dimer, and other than a resolution of the $g_\perp$ transition into two components, the spectrum of the pyrazine bridged mixed valence compound yields a comparable $g_\perp$ value of 2.66. Furthermore, the line-widths of the resonances bands of the [III,III] and [II,III] compounds are comparable. These results were said to indicate that the presence of a ruthenium ion at one end of a pyrazine bridge did little or nothing to perturb the ruthenium(III) on the other end of the bridging ligand, and to verify the conclusion that the mixed valence compound belongs to Class II. A line-width study was interpreted in terms of a rate of electron transfer slower than 10^9 sec^{-1}. An NMR study showed that the rate was greater than 10^5 sec^{-1}. Thus, from the Arrhenius equation, the energy barrier lies between 3.4 kcal $mole^{-1}$ and 6.7 kcal mol^{-1}. Hush disagrees and described a delocalized model and new EPR data in his presentation at the Institute.[111]

A Mixed Valence Cobalt-Copper Complex. Kahn and coworkers[62-64] have investigated a series of heterometallic systems of the general formula NM'L where the ligand is the anion of the N,N'-bis(2-hydroxy-3-carboxybenzylidene)-1,2-diamminoethane:

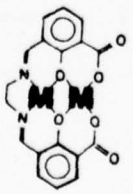

(25)

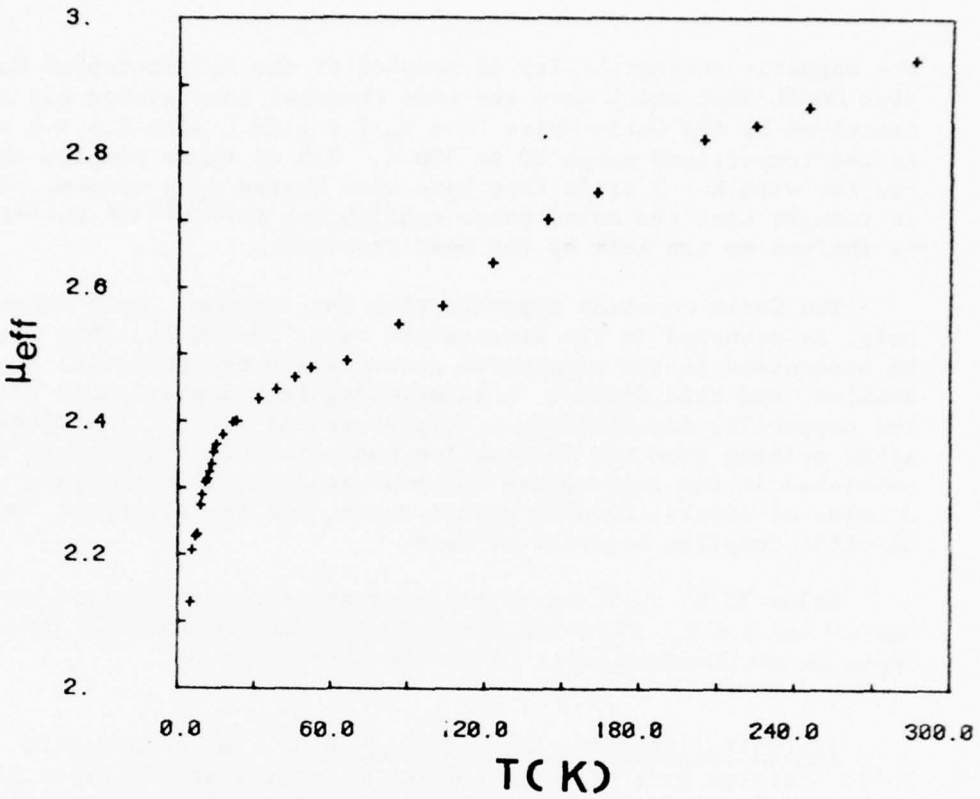

Figure 5. The temperature variation of the magnetic moment of $[\{Ru(NH_3)_5\}_2 \text{ pyrazine}]^{6+}$.

The magnetic susceptibility of samples of the cobalt-copper complex $CoCuL \cdot 3H_2O$ which have the same chemical composition may be described by the Curie-Weiss laws $\chi_m \cdot T = 1.69\ k$ with $0.4 < k < 1$ in the temperature range 30 to 300 K. All of these samples obey the law with $k = 1$ after they have been heated in a vacuum. It is thought that the solid phase equilibrium $Co^{II}Cu^{II} \rightleftharpoons Co^{III}Cu^{I}$ is shifted to the left by the heat treatment.

The Curie constant suggests that the triplet spin state, only, is occupied in the temperature range 30-300 K. This may be understood if the single-ion ground state of cobalt(II) is a doublet, and this doublet is interacting ferromagnetically with the copper(II) ion yielding a triplet ground state. The singlet state arising from the interaction must lie much too high to be populated in the temperature interval studied, thus implying a J value of several hundred wave numbers, and the strongest ferromagnetic coupling reported to date.

Below 30 K, $\chi_m \cdot T$ decreases and reaches the value 1.55 $cm^3\ mole^{-1}$ at 3.6 K. This low temperature behavior probably arises from an antiferromagnetic intermolecular coupling.

$[Fe(II)Fe(III)_2(CH_3COO)_6O(H_2O)_3] \cdot 2H_2O$. The trimetallic basic acetates have been the subject of many investigations of exchange dating from the classical work of Welo[65] and Kambe.[3] Lupu[66] has prepared and studied iron(II)iron(III) mixed valence basic acetate compounds. From magnetic susceptibility data in the temperature range 94-296 K, he found the exchange coupling constant between the iron(III) ions to be $-36\ cm^{-1}$, a value which is comparable to that found for the iron(III) basic acetates. However, the exchange integral between the iron(II) and iron(III) ions was found to be temperature dependent, being $2.8\ cm^{-1}$ at 100.7 K and $-10\ cm^{-1}$ at 288 K. This behavior was attributed to changes in bond distances. As Lupu suggested, more extensive magnetic studies should be carried out on these interesting compounds. Brown and co-workers have made such measurements;[108] they found J[Fe(II)-Fe(III)] to be $-50\ cm^{-1}$, J[Fe(III)-Fe(III)] to be $-14.5\ cm^{-1}$, and both coupling constants to be temperature independent.

Mössbauer studies on $[Fe(II)Fe(III)_2(CH_3COO)O(H_2O)_3] \cdot 2H_2O$ and $[Fe(II)Fe(III)_2(CH_3COO)O(py)_3] \cdot 0.5$ py show that the iron ions are indistinguishable on the Mössbauer time scale at room temperature, but are readily distinguishable below 200 K.[67] These data, along with optical absorption spectra, support the assignment of these compounds to class II.

Triangular Cobalt Clusters. The compounds $Co_3(h^5\text{-}C_5H_5)_3S_2$, $Co_3(h^5\text{-}C_5H_5)_3(CO)S$, and $[Co_3(h^5\text{-}C_5H_5)_3S_2]I$ have structures consisting of three metal ions in a triangular array which are capped above and below by the two sulfur atoms or by one sulfur atom and the carbonyl groups, with the cyclopentadienyl ions bonded to

the cobalt atoms.[68] These three compounds exhibit a fascinating array of magnetic properties. $Co_3(h^5\text{-}C_5H_5)_3(CO)S$ is diamagnetic, and the monoxidized iodide salt is a simple paramagnet with a magnetic moment which decreases linearly from 1.95 μ_B at 297 K to 1.77 μ_B at 83 K. At temperatures greater than 195 K the magnetic susceptibility of the disulfide complex obeys the Curie-Weiss law, but at 195 K there is an abrupt discontinuity and the magnetic susceptibility decreases to approximately one-half of its maximum value within a 30° temperature range. Additional evidence for a phase transition at 192.5 K is provided by the calorimetric study by Sorai and coworkers.[69]

A ^1H magnetic resonance study of a CS_2 solution of the disulfide complex over the temperature range 163 to 324 K revealed three distinct regions of paramagnetic shift dependence. For $T > 260$ K the paramagnetic shift varies as $1/T$ and $S = 1$; below 173 K the shift is zero as expected for a diamagnetic substance; while in the region $173 < T < 260$, the shift reflects the spin state equilibrium. However, the shift data can be fit by the expression for the thermal equilibrium between singlet and triplet species only if a temperature dependent energy separation is used.

Cubane Type Cluster Systems Containing Iron. Tetrametallic cubane type cluster systems containing iron have been of considerable interest since it is known that a distorted cubic cluster Fe_4S_4 is present in some non-heme iron-sulfur proteins, and complexes of the type $[(RS)FeS]_4^{n-}$ (where RS is an alkyl or aryl mercaptide) have been shown to be close structural and electronic analogues of the proteins.[70] The Fe_4S_4 cubane structure is also present in dithiolene complexes[71] of the type $[\{(CF_3)_2C_2S_2\}FeS]_4^{n-}$, and in cyclopentadienyl complexes of the type[72] $[(h^5\text{-}C_5H_5)FeS]_4^{n-}$. An analogous tetrametallic complex with CO replacing the bridging sulfur atoms is also known.[73]

In the reduction of $[(SR)FeS]_4^{2-}$ to the trianion, there are significant changes in the Mössbauer isomer shifts, quadrupole interactions, and magnetic hyperfine interactions at the iron sites. These properties have been interpreted in terms of a molecular orbital delocalized over the four metal ions. In the dithiolene complexes $[(R_2C_2S_2)FeS]_4^{2-}$, there are only small changes in the Mössbauer parameters. This observation indicates that the orbital to which the electron is added is predominately ligand based. Oxidation of $[(h^5\text{-}C_5H_5)Fe(CO)]_4$ to the monocation results in a change in the quadrupole interaction and a small magnetic hyperfine interaction, but there is no change in the isomer shift. These results suggest that the electron is removed from an orbital with some metal as well as ligand character.[74]

The electron distribution in the series $[(h^5\text{-}C_5H_5)FeS]_4^{n+}$

(n = 0, 1, 2) is very complex. Mössbauer spectra consist of single quadrupole doublets indicating that all iron atoms are identical on the Mössbauer time scale. The puzzling feature is that the mono-and dication exhibit the same electric quadrupole splittings even though there are significant changes in the iron-sulfur bond distances in going from the neutral molecule to the cations.[75] Reiff and coworkers conclude that the "invariance of the isomer shift upon oxidation from the [neutral molecule] to the [dication] suggests either that electrons are removed from ligand-based orbitals with no change in metal 3d, 4s population or that the electrons are removed from metal-based molecular orbitals in the successive oxidations... and that in the resulting products... there is a redistribution of ligand electron density to the metal atoms so as to result in little overall change of metal orbital electron population."

Magnetic data for the mono-and dications are given in Table V, where it may be seen that both compounds are paramagnetic and that the magnetic moment decreases as the temperature decreases.

Table V. *Magnetic Data for* $[(h^5\text{-}C_5H_5)FeS]_4^{+/2+}$

$[CpFeS]_4^+$		$[CpFeS]_4^{2+}$	
T,K	μ_B	T,K	μ_B
303	1.33	298	0.80
276	1.23	288	0.78
255	1.20	252	0.73
232	1.16	216	0.68
190	1.07	180	0.62
131	0.95	144	0.57
99	0.87	108	0.53
52	0.77	78	0.48
25	0.67		
11.2	0.59		
4.2	0.52		
2.14	0.45		
1.50	0.41		

A magnetic moment of 0.87 μ_B/Fe would be expected for one unpaired electron in the monocation cluster, i.e. 1.73 $\mu_B/\sqrt{4}$; the high moments above 100 K indicate that higher cluster spin states are occupied, while the decrease in magnetic moment at low temperatures suggests an antiferromagnetic intercluster interaction. The magnetic behavior of the dication suggests that paramagnetic

states are being occupied, but Reiff and coworkers noted that a large TIP contribution could not be ruled out. It is clear that the electronic structures of these clusters are affected by the terminal as well as the bridging ligands. These effects can be rationalized by qualitative molecular orbital calculations,[75b] but more powerful calculations as well as more experimental data are needed before the behavior of these important class III clusters can be thoroughly understood.

Di-μ-acetato-tetrakis[μ_3-methoxo-2,4-pentanedionatocobalt-(II,III)]. A mixed valence compound containing cobalt(II) and cobalt(III) may be prepared by the oxidation with hydrogen peroxide of a mixture of cobalt(II) acetate, 2,4-pentanedione, and potassium hydroxide.[76] The cluster has a cubane type structure with cobalt ions and methoxide oxygen atoms at alternate corners of the cube, and quasi-octahedral coordination of the cobalt ions is completed by a chelated 2,4-pentanedionato group and by an oxygen of one of the acetate groups which bridge the top and bottom faces of the cube. Since the cobalt-oxygen bond distances for one pair of these cobalt ions are 0.16-0.20 Å shorter than those of the second pair, it is likely that the former are the cobalt(III) ions.

The magnetic moment of the cluster is temperature dependent, being 4.98 μ_B per cobalt(II) at room temperature and 4.62 μ_B at 77°K. Although the geometry might suggest a class I system containing a pair of exchange coupled cobalt(II) ions, the dark brown color of the material makes such a classification suspect.

One-Dimensional Chains

Partially Oxidized Metallophthalocyanines. Reactions of Fe, Co, Ni, Cu, Zn, Pt and metal-free phthalocyanines with iodine vapor or solutions in solvents such as chlorobenzene yield darkly colored solids of the general formula M(phthalocyanine)I_x, where x can take on values from less than one to nearly four, depending on reaction conditions and the phthalocyanine.[77a] The mixed valence character of these materials has been established by resonance Raman data which shows that the iodine is present as I_3^-, by iodine-129 Mössbauer studies, and by X-ray structural studies on Ni(phthalocyanine)$(I_3)_{.33}$. The $[Ni(Pc)]^{0.33+}$ molecules stack to form one-dimensional chains, and the I_3^- molecules are present as disordered chains in channels formed by the phthalocyanine units.[77b] The electrical conductivity measured along the stacking direction (the crystallographic c axis) for $[Ni(Pc)](I_3)_{.33}$ is in the range 250-650 ohm^{-1} cm^{-1}, values which are comparable to the electrical conductivities of the most highly conductive molecular materials yet reported.[78] The electrical conductivity increases as the temperature decreases until a maximum value of $\sigma(T)/\sigma_{RT}$ of about four is reached near 90 K at which point there

is an abrupt drop in conductivity. Remarkably, there is no sharp break in the magnetic susceptibility, which is weakly paramagnetic and increases with temperature, coincident with the "metal-insulator" transition.

Iridium Carbonyl Chloride. For a number of years it was thought that the compound originally characterized as $Ir(CO)_3Cl$ was nonstoichiometric,[79-82] but recent work by Reiss, Hagley, and Peterson has confirmed the initial formulation.[83] The chlorotricarbonyliridium(III) units of $Ir(CO)_3Cl$ stack in a staggered manner with an Ir-Ir distance of 2.844 (1) A and an Ir-Ir-Ir angle of 178.53 (2)°. While it is true that data from physical measurements on the stoichiometric material are yet to be had, the data reported by Ginsberg and coworkers[82] on their samples are very interesting. It is likely that these latter workers were carrying out measurements on a mixed valence compound, whose identity is yet to be established. A detailed discussion of the experimental observations including Mossbauer and magnetic susceptibility must await the completion of this task.

Perylene-Metal Dithiolate Complexes. Ion-radical complexes of the general formula $(perylene)_2M(mnt)_2$ (where M = Ni, Cu, Pd, Pt and mnt = maleonitriledithiolate) exhibit relatively high electrical conductivities. The magnetic properties of these compounds have been investigated in attempts to understand the electronic structure of the constituents and to identify the conduction pathways.[84-86] A study of the temperature dependence of the EPR spectrum of $(perylene)_2Pd(mnt)_2$ revealed that the paramagnetism was associated with two spin subsystems, and that each of these is exchange coupled either pairwise or in linear stacks. The magnetic susceptibility data for the copper complex suggested that the $Cu(mnt)_2$ sites were not completely in the monoanionic form, thus implying that the average charge on the perylene sites is less than +1/2. An analysis of the susceptibility data in terms of the contributions from the constituents showed that the magnetic susceptibility of the perylene spin system was largely temperature independent over the range 100-300 K but increased abruptly at 77 K in a manner similar to the temperature dependence of the magnetic susceptibility of other conducting salts such as quinolinium $(TCNQ)_2$. The magnetic moment per formula unit of $Cu(mnt)^{n-}$ was found to be 0.85 μ_B while that of $Ni(mnt)^{n-}$ was 1.99 μ_B. For $Pd(mnt)^{n-}$ it was estimated that there were 0.145 monoanions per formula unit.

$K_2Pt(CN)_4Br_{0.3}\cdot 3H_2O$. The magnetic susceptibility of a single crystal of KCP(Br) has been reported by Menth and Rice.[87] χ is independent of temperature and equal to -160×10^{-6} cm^3mole^{-1}, a value which is very close to that expected for the diamagnetism of the constituent atoms in view of the measured diamagnetic susceptibility of -136×10^{-6} cm^7mole^{-1} for $K_2Pt(CN)_4\cdot H_2O$.[88]

χ is temperature dependent and in the temperature range 4.2 to 40 K may be described by the expression

$$\chi_{||} = -100 \times 10^{-6} + \frac{1.83}{T} \times 10^{-4}$$

In the temperature range 40 to 250 K the expression for $\chi_{||}$ is

$$\chi_{||} = -160 \times 10^{-6} + \frac{2.50}{T} \times 10^{-3}$$

The need for two Curie-Weiss laws to describe the temperature dependence of the magnetic susceptibility also arises for iridium carbonyl chloride and $(H_3O)_{1.6}[Pt(C_2O_4)_2]\ nH_2O$.

Menth and Rice proposed an interrupted strand model for $\chi_{||}$ of the form

$$\chi_i = 1/2N(\varepsilon_F)\left[\frac{\mu_B g_i}{2}\right]^2 + \frac{1}{2}\left[\frac{Na}{l_o}\right]\left[\frac{1}{k_B T}\right]\left[\frac{\mu_B g_i}{2}\right]^2 \qquad (26)$$

where $N(\varepsilon_F)$ is the thermal density of states at the Fermi energy, N_a is the number of strands per unit area perpendicular to the strand axis, and l_o is the mean length of the 1-D metallic boxes which are formed by the random distribution of lattice defects along the strand. The expression for χ is valid for $k_B T << \Delta$, where $\Delta \simeq 2N_a/(N(\varepsilon_F)l_o)$. Δ is the mean spacing of the energy levels within the box in the vicinity of the Fermi energy.

The first term in the expression represents the Pauli contribution which arises from the boxes which have an even number of carriers and which may be estimated. In a 1-D structure $N(\varepsilon_F) = 2N_a/\pi v_F$, where for KCP(Br) $N_a \sim 10^{14}$ cm^{-2} and $v_F \sim 10^8$cm sec^{-1}. Substitution yields $\chi_p \sim 5 \times 10^{-6}$cm^{3}mole^{-1}.

The second term in expression 26 arises from the boxes which have an odd number of carriers. In principle, it should be possible to deduce l_o, but the result was thought to be unreasonably large. Also, the fraction of unpaired spins per platinum site, f, may be estimated from the expression $\chi = n_s\left[\frac{\mu_B g}{2}\right]^2 f/k_B T$, where n_s is the number of platinum sites per unit volume. For $T < 40$, $f \simeq (2/g_{||})^2 \times 0.6 \times 10^{-3}$, and for $T > 40$, $f \simeq (2/g_{||})^2 \times 7 \times 10^{-3}$. This parameter was thought to be unrealistically small, and it must be concluded that this model is not applicable to KCP(Br).

Kuindersma and Sawatzky have also measured the magnetic susceptibility of KCP(Br) and attributed the Curie behavior at low temperature to the presence of impurity platinum ions in which the d_{xz}, d_{yz} orbitals are the highest occupied orbitals.[89] They argued that the model used by Menth and Rice was inappropriate and that a tight binding model would have been preferable. They suggested that the electrons were strongly paired and that a possible explanation may be found in terms of a semiconductor model, where the band gap was much larger than 300 K. No details on this proposal have been presented.

Phillips[90] has suggested that the abrupt change in slope of the Curie-Weiss plots is a third order phase transition which is intrinsic and is associated with a lateral alignment of paramagnetic domain tips. Along a given metal chain in KCP(Br), or iridium carbonyl chloride, or $(H_3O)_{1.6}[Pt(C_2O_4)_2]nH_2O$ there are quasi periodic microdomains which may have localized spins associated with electrons in tip states. At high temperatures these spins are uncorrelated, but at low temperatures interchain alignment may become possible.

$(H_3O)_{1.6}[Pt(C_2O_4)_2]nH_2O$. Magnetic susceptibilities of polycrystalline, partially oxidized samples of $(H_3O)_{1.6}[Pt(C_2O_4)_2]nH_2O$ with two different values of n, and the unoxidized potassium salt have been measured in the temperature range 1.5 - 300 K.[91] The potassium salt is diamagnetic as expected, while the partially oxidized acids are diamagnetic down to 15-20 K at which point they become paramagnetic. Two Curie-Weiss laws are required to fit the temperature dependence of the magnetic susceptibility. The sample with a relatively large water content has a magnetic moment of 0.097 μ_B above 17 K and the moment is 0.079 μ_B below 17 K. The corresponding values for the sample with a relatively small water content are 0.11 μ_B above 22 K and 0.097 μ_B below 22 K. It is thought that unusual magnetic behavior of these compounds are characteristic of linear chain, metal-metal bonded, partially oxidized systems. The paramagnetic behavior may arise from defects or localized singly occupied states, but no explanation has been put forth for the abrupt change in slope of the Curie-Weiss plots.

Random Exchange in Quinolinium $(TCNQ)_2$. Quinolinium $(TCNQ)_2$ is a charge transfer compound consisting of separated stacks of quinolinium ions and TCNQ ions. The very high electrical conductivity of the material has attracted a great deal of attention and a number of elegant studies have been described in the literature. The magnetic properties are of especial interest. At relatively high temperatures the magnetic susceptibility is essentially constant, but at low temperatures there is a Curie-like tail. Azevedo and Clark[21] have been successful in treating the magnetic behavior of quinolinium $(TCNQ)_2$ using the Bulaevskii

model for a random exchange Heisenberg chain with a density of states having the form $\rho(\varepsilon) = Ak^{(\alpha-1)}|\varepsilon|^{-\alpha}$, where A and α are parameters selected to fit the data. The best fit of the magnetic susceptibility data to the Bulaevskii model yield A = (1.81 ± 0.1) x 10^{-3} $K^{\alpha-1}$ and α = 0.82 ± 0.01. If one takes these values and integrates the density of states equation, a 3% molar concentration of spins with ε/k < 10 K is obtained. The other 97% of the spins must be involved in exchange interactions for which J/k > 10 K. A detailed description of the susceptibility follows from the specific form of $\rho(J)$ given above.

Two Dimensional Sheets

Potassium Copper Sulfide, KCu_4S_3. The mixed valence compound KCu_4S_3, which contains three copper ions in formal oxidation state +1 and one copper ion in formal oxidation state +2, has a layered structure of sulfur bridged copper ions where the layers are separated by potassium ions.[92,93] The copper ions are tetrahedrally coordinated by sulfur atoms, and with all copper ions are equivalent. The tetrahedra form the layers by sharing edges and vertices in this Class IIIB compound.

The conductivity of pressed pellets of KCu_4S_3 is 4.1 ± 1.1 x 10^3 $ohm^{-1}cm^{-1}$ at room temperature and rises to 6.1 x 10^4 ohm^{-1} cm^{-1} at 18 K. Although it has not been possible to obtain crystals for complete anisotropic measurements, the conductivity in the plane has been measured at room temperature and is ∿ 8 x 10^3 $ohm^{-1}cm^{-1}$. As expected, this metallic material possesses a very small paramagnetic susceptibility that is nearly temperature independent. Below 15 K there is an increase in susceptibility which follows the Curie Weiss law with C = 0.00477 and θ = 0.16. This behavior suggests the presence of a small concentration of paramagnetic sites, either defects or paramagnetic impurities. If the Curie-Weiss paramagnetism is subtracted from the observed magnetic susceptibility, then a residual molar susceptibility of ∿ 7 x 10^{-5} cgs $mole^{-1}$ results. This is a sum of second order single ion TIP and Pauli paramagnetism, and it is difficult to evaluate either of these independently.

Layered Transition Metal Dichalcogenides. Layered transition metal dichalcogenides such as 2H...TaS_2 and 2H...$NbSe_2$ may be readily intercalated with organic molecules, metal atoms, and other σ donors. The intercalated substances frequently have higher superconducting transition temperatures than the precursors, but in some cases the transition temperature is shifted to lower values. Hydrogen may be intercalated in 2H...TaS_2, 2H...$NbSe_2$, 2H...NbS_2, and TiS_2 (but not in 1T...TaS_2, HfS_2, ZrS_2, or MoS_2) by electrolysis in acid solution.[94] In these compounds hydrogen acts as an electron donor.

Magnetic susceptibilities of 2H...TaS_2 and four hydrogen intercalated compounds H_xTaS_2 are given in Figure 6. There is a marked decrease in χ_g for 2H...TaS_2 near 80 K. This decrease in magnetic susceptibility, which is caused by superlattice formation, is suppressed by hydrogen intercalation and is absent when $X \geq 0.11$. Some pertinent magnetic data are summarized in Table VI, where it may be seen that the compound with the highest superconducting transition temperature (X = 0.11) shows the smallest, positive $\Delta\chi$. It is thought that the bonding is due to charge transfer from hydrogen to the *d* band of the tantalum sulfide layer, and that the enhancement of the superconducting transition temperatures is due to a suppression of a charge density wave near 80 K.

Table VI. *Magnetic Properties and T_c of Tantalum Sulfides*

Compound	χ(max) x 10^6 emu/g	$\Delta\chi$ [χ(max)-χ(4.2)]	T_c, K
2H...TaS_2	+.725	+0.134	0.8
$H_{0.06}TaS_2$	+.622	+0.078	
$H_{0.09}TaS_2$	+.590	+0.020	
$H_{0.11}TaS_2$	+.606	+0.002	4.2
$H_{0.15}TaS_2$	+.523	-0.003	
$H_{0.87}TaS_2$	(-0.190)	0	<0.5
$Ta_{1.05}S_2$	+.472	+0.050	∿3.6

None of the H_xTiS_2 compounds were superconducting above 0.5K, and the compound H_xNbSe_2 with $x = 0.01$ exhibited an enhancement in T_c of 0.2 K (to 7.45 K); while for the compound with $x = 0.2$, T_c was less than 0.5 K. 2H...$NbSe_2$ also has a distortion at about 35 K, which is suppressed by intercalation.

Three-Dimensional Polymers

Prussian Blue. The mixed valence compound $Fe(III)_4[Fe(II)(CN)_6]_3 \cdot 14H_2O$ has been a frequent object of study.[95] In this compound the iron(II) ion, being coordinated by six carbon atoms, occupies a strong-field octahedral site, while the iron(III) ions are in two different kinds of weak-field sites. In one of these high spin iron(III) ions are coordinated by six nitrogen atoms from the cyano ligands coordinated to the iron(II) ions, while in the second site the high spin iron(III) ions are coordinated

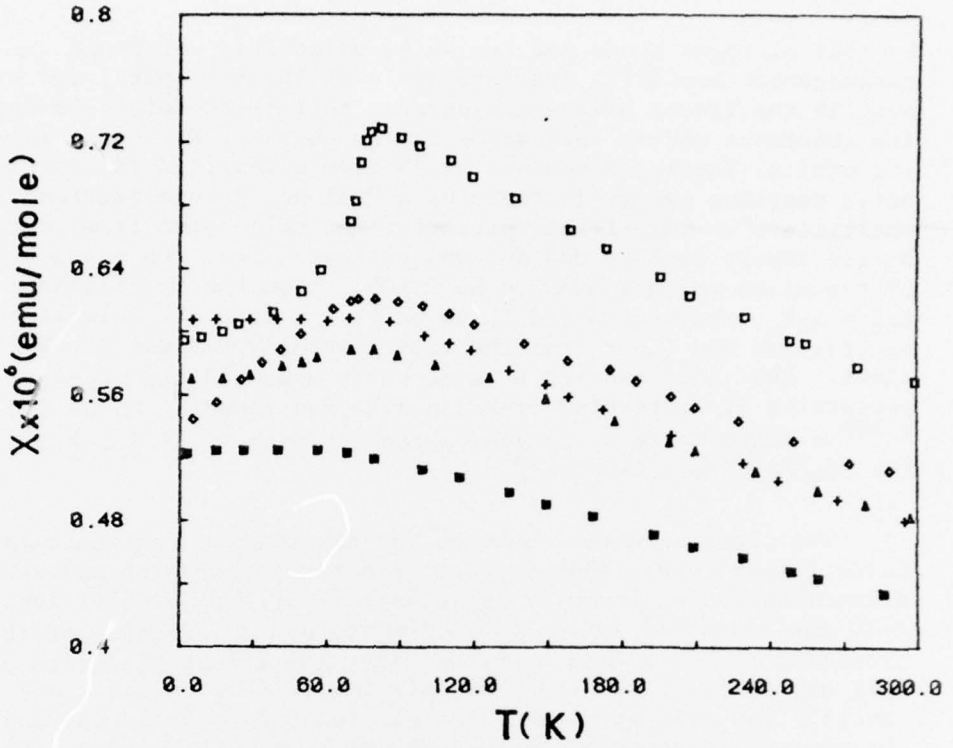

Figure 6. Magnetic susceptibility data for 2H...TaS_2 (□), $H_{0.06}TaS_2$ (◇), $H_{0.09}TaS_2$ (△), $H_{0.11}TaS_2$(+), $H_{0.15}TaS_2$ (■).

by four nitrogen atoms and two water molecules. Although the paramagnetic iron(III) ions are at least 10.16 Å apart, and present in the linear bridge arrangement Fe(III)-NC-Fe(II)-CN-Fe(III), the substance orders ferromagnetically above 5 K. Using molecular orbital theory, Mayoh and Day[96] have calculated the ferromagnetic coupling energy in terms of a "valence delocalization coefficient". This latter parameter was calculated from perturbation theory to be 0.083 and was estimated from the intensity of the mixed valence band to be 0.106. From the relationship $E_{fm} \sim k_B T_c$, they estimated T_c to be 11.2 K from the calculated coefficient and 6.6 K from the experimentally estimated coefficient. Ludi and coworker have recently measured the magnetic properties of deuterated Prussian blue and found T_c to be 5.6 $\pm$0.1 K,[109] a value which is in good agreement with T_c of 5.5 $\pm$ 0.5 K for $Fe_4[Fe(CN)_6]_3 \cdot 14H_2O$.[110]

The close agreement between the experimental and calculated Curie temperatures lends support to a mechanism which involves delocalization of formally t_{2g} electrons of the iron(II) ions onto the iron(III) ions. Since the t_{2g} and e_g orbitals of the iron(III) ions are half occupied, they may accept electrons of only one spin. Since there are six iron(III) ions about a given iron(II) ion, the spins of these six ions are correlated, and the process is repeated throughout the lattice. Mayoh and Day[96] calculated the energy per each iron(II) center when the spins of the six neighboring iron(III) ions were all arranged parallel to one another, and when the six spins were arranged randomly, and attributed that energy to the ferromagnetic coupling energy. The recent prediction[97] of a very low ordering temperature in voltaite[98] demonstrates the power of the computational technique.

Iron Fluoride Dihydrate. Brown, Reiff and coworkers[99] have made Mössbauer and magnetic susceptibility measurements on $Fe_2F_5 \cdot 2H_2O$ which show that the material orders ferrimagnetically at 48 K. Above the critical temperature distinct quadrupole-split Mössbauer absorptions were observed for both the iron(II) and the iron(III) sites. These observations demonstrate the nonequivalence of the oxidation states and establish $FeF_5 \cdot 2H_2O$ as a class II mixed valence compound. Ferrimagnetic ordering was established by the observation of spontaneous magnetization, field-dependent susceptibilities, and a saturation moment corresponding to a formula unit spin of S = 1/2. Below the critical temperature the Mössbauer spectra exhibit the magnetic hyperfine structure expected for ferrimagnetic ordering.

The magnetic susceptibility data above the Néel temperature are plotted as χ^{-1} versus temperature in Figure 7, where the solid line is the best fit to the equation for the Néel hyperbola

$$\chi^{-1} = (T-T_c)(T-T_c')/[C(T-\theta')]$$

with the parameters T_c = 48 K, T_c' = -200.9 K, θ' = 25.8 K, and C = 6.74. At high temperatures the Néel hyperbola asymptotically

approaches Curie-Weiss behavior, and at the ferrimagnetic Néel temperature the hyperbola becomes infinite. For $Fe_2F_5 \cdot 2H_2O$, the limiting high-temperature magnetic susceptibility obtained from a fit of the Curie-Weiss law to data in the temperature range 200-250 K is given by $\chi = 6.74/(T+179)$. The effective magnetic moment calculated from $\mu_{eff} = 2.828\ C^{1/2}$ is 7.34 μ_B, a value to be compared to the moment of 7.68 μ_B which is predicted for two noninteracting high spin iron(II) and iron(III) ions with g = 2. The negative θ in the Curie-Weiss law implies antiferromagnetic interactions between Fe(II) and Fe(III).

Below the Néel temperature long range order is expected for ferrimagnetic materials, and, as expected, $Fe_2F_5 \cdot 2H_2O$ exhibits spontaneous magnetization in zero applied field. Qualitatively the behavior agrees with that predicted by a Brillouin function with S = 1/2 and provides additional evidence for ferrimagnetic ordering. Finally, the saturation moment is 1.2 μ_B. For a negative coupling constant between Fe(II) and Fe(III), a saturation moment of 1.0 μ_B would have been expected, while a positive coupling between these ions would yield S = 9/2 and a saturation moment of 9 μ_B.

Iron Fluoride Heptahydrate, $Fe_2F_5 \cdot 7H_2O$. The magnetic susceptibility of a powdered sample of $Fe_2F_5 \cdot 7H_2O$ has been measured as a function of temperature using a vibrating sample magnetometer operating at 10 kOe.[100] A transition to an antiferromagnetic state was observed at 3.0 $\pm$ 0.2 K. Using data collected in the range 4.2 - 60 K, a magnetic moment of 7.68 μ_B and a Weiss constant of 6.9 K may be calculated. This is precisely the magnetic moment expected from the spin-only values of the two iron ions. Although ferrimagnetism may have been expected, no spontaneous magnetization was observed below T_N, so the authors proposed a four-sublattice model to account for the observed behavior. Additional measurements are needed in order to sort out the interactions in this mixed valence compound since the Mössbauer and spectroscopic results of Brown and coworkers[101] lead to the conclusion that $Fe_2F_5 \cdot 7H_2O$ is a class I material.

Chevrel Phase Compounds. Compounds of the general formula $M_xMo_6S_8$ with M = Cu, Pb, Sn, Ag, rare earths, etc., which were first reported by Chevrel et al.[102] have attracted considerable attention since they undergo a transition to a superconducting state.[103] The structure of these compounds consist of Mo_6S_8 units with the second metal atom occupying positions between the clusters. The identity and concentration of the second metal atom has a dramatic effect on T_c.[104,105] The rare earth molybdenum sulfides $(RE)_xMo_6S_8$ ($x \sim 1$ for the light rare earths and $x \sim 1.2$ for the heavier ones) are superconducting even in the presence of a high concentration of magnetic ions. Extensive magnetization measurements have been reported for the series of

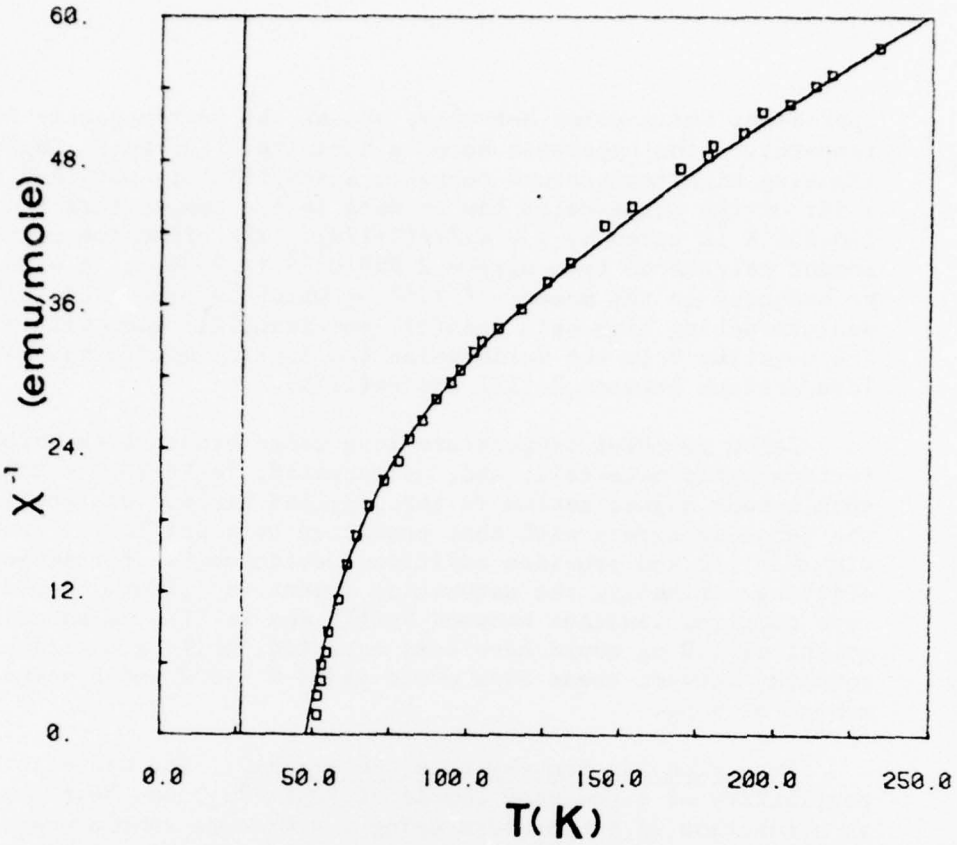

Figure 7. Magnetic susceptibility data for $Fe_2F_5 \cdot 2H_2O$. The solid line is the best fit of Néel hyperbola to the experimental data.

compounds $(RE)_xMo_6Se_8$ ($x \sim 1$; RE = La, Ce, Pr, Eu, Gd, Yb, and Lu).[106] The susceptibilities of $CeMo_6Se_8$, $PrMo_6Se_8$, and $YbMo_6Se_8$ deviate marked from Curie-Weiss behavior above 10 K because of crystal field effects. There is a small exchange interaction between gadolinium ions in superconducting $Gd_{1.2}Mo_6Se_8$ which leads to long range order at 0.8 K but $CeMo_6Se_8$, which apparently becomes ferromagnetic, does not superconduct above 0.05 K. The compound $Er_xMo_6Se_8$ undergoes a transition to a superconducting state at T_c = 5.70 - 6.17 K, and the Er^{3+} ions order antiferromagnetically at 1.07 K. The ordering does not result in the loss of superconductivity.[107] These compounds provide very good examples of substances which exhibit coexisting superconductivity and long range order.

ACKNOWLEDGEMENTS

This work was supported in part by the Office of Naval Research and by the North Atlantic Treaty Organization.

REFERENCES

1. Cohen, I. Structure and Bonding, in press.
2. Robin, M.B.; Day, P. Adv. Inorg. Chem. And Radiochem. 1967, 10, 247.
3. Kambe, K. J. Phys. Soc. Japan 1950, 5, 48.
4. Hatfield, W.E. In "Theory and Applications of Molecular Paramagnetism", Boudreaux, E.A. and Mulay, L.N., Ed.; Wiley: New York, 1976; Chapter 7, pp. 349ff.
5. Kudo, T.; Matsubara, F.; Katsura, S. Physica 1978, 93A, 255.
6. Wrobleski, J.T.; Brown, D.B. Inorganic Chemistry, in press.
7. Fisher, M.E. J. Math. Phys. 1963, 4, 123.
8. Onsager, L. Phys. Rev. 1944, 65, 90.
9. Katsura, S. Phys. Rev. 1963, 129, 2835.
10. Fisher, M.E. Am. J. Phys. 1964, 32, 343.
11. Bonner, J.C.; Fisher, M.E. Phys. Rev. 1964, 135A, 640.
12. Weng, C.-Y Ph. D. Dissertation, Carnegie-Mellon University, 1968.
13. Wagner, G.R.; Friedberg, S.A. Phys. Lett. 1964, 9, 11.
14. Rushbrooke, G.S.; Wood, P.J. Molec. Phys. 1958, 1, 257.
15. Smart, J.S. "Effective Field Theories of Magnetism", Saunders: Philadelphia, 1966.
16. DeJongh, L.J.; Miedema, A.R. Adv. Phys. 1974, 23, 1.
17. Van Vleck, J.H. "The Theory of Electric and Magnetic Susceptibilities"; Oxford University Press: London, 1932.
18a. Hall, J.W. Ph.D. Dissertation, University of North Carolina, Chapel Hill, 1977; b. Jotham, R.W. J. Chem. Soc. Dalton Trans. 1977, 266.
19. Bulaevskii, L.N.; Zvarykina, A.V.; Karimov, Yu. S.; Lyubovskii, R.B.; Shchegolev, I.F. Sov. Phys.-JETP 1972, 35, 384.
20. Theodorou, G.; Cohen, M.H. Phys. Rev. Lett. 1976, 37, 1014.
21. Azevedo, L.J.; Clark. W.G. Phys. Rev. B 1977, 16, 3252.
22. Dupas, A.; LeDang, K.; Renard, J.P.; Veillet, P.; Daoud, A.; Perret. R. J. Chem. Phys. 1976, 65, 4099.
23. Oguchi, T. J. Phys. Soc. Japan, 1971, 31, 1021, and references therein.
24. Yamada, I. J. Phys. Soc. Japan, 1972, 33, 979.
25. Erdos, P. J. Phys. Chem. Solids, 1966, 27, 1705 and references therein.
26. Néel, L. Ann. Phys. (Paris) 1948, 3, 137.
27. Craik, D.J. "Magnetic Oxides"; Wiley: New York, 1975.
28. Quickenden, T.I.; Marshall, R.C. J. Chem. Educ. 1972, 49, 114.
29. Mulay, L.N. in "Theory and Applications of Molecular Paramagnetism", Boudreaux, E.A. and Mulay, L.N., Ed.; Wiley: New York, 1976; Chapter 9.
30. Bennett, L.H.; Page, C.H.; Swartzendruber J. Research, National Bureau of Standards, 1978, 83, 9.
31. Nyholm, R.S.; Turco, A. Chem. Ind. (London) 1960, 74.
32. Plaskin, P.M.; Stoufer, R.C.; Mathew, M.; Palenik, G.J. J. Am. Chem. Soc. 1972, 94, 2122.

33. Cooper, S.R.; Calvin, M. J. Am. Chem. Soc. 1977, 99, 6623.
34. Cooper, S.R.; Dismukes, G.C.; Klein, M.P.; Calvin, M. J. Am. Chem. Soc. 1978, 100, 7248.
35. Boucher, L.J.; Coe, C.G. Inorg. Chem. 1976, 15, 1334 and references therein.
36. Cowan, D.O.; Kaufman, F. J. Am. Chem. Soc. 1970, 92, 219.
37. Kaufman, F.; Cowan, D.O. J. Am. Chem. Soc. 1970, 92, 6198.
38. Hush, N.S. Prog. Inorg. Chem. 1967, 8, 391.
39. Cowan, D.O.; Candela, G.A.; Kaufman, F. J. Am. Chem. Soc. 1971, 93, 3889.
40. Sohn, Y.S.; Hendrickson, D.N.; Gray, H.B. J. Am. Chem. Soc. 1970, 92, 3233.
41. Maki, A.H.; Berry, T.E. J. Am. Chem. Soc. 1965, 87, 4437.
42. LeVanda, C.; Bechgaard, K.; Cowan, D.O.; Rausch, M.D. J. Am. Chem. Soc. 1977, 99, 2964.
43. Cowan, D.O.; LeVanda, C. J. Am. Chem. Soc. 1972, 94, 9271.
44. Mueller-Westerhoff, U.T.; Eilbracht, P. J. Am. Chem. Soc. 1972, 94, 9272.
45. Cowan, D.O.; LeVanda, C.; Collins, R.L.; Candela, G.A.; Mueller-Westerhoff, U.T.; Eilbracht, P. J.C.S. Chem. Comm. 1973, 329.
46. Mueller-Westerhoff, U.T.; Eilbracht, P. Tetrahedron Letters 1973, No. 21, 1855.
47. LeVanda, C.; Bechgaard, K.; Cowan, D.O.; Mueller-Westerhoff, U.T.; Eilbracht, P.; Candela, G.A.; Collins, R.L. J. Am. Chem. Soc. 1976, 98, 3181.
48. Davison, A.; Smart, J.C. J. Organomet. Chem. 1973, 49, C43.
49. Smart, J.C.; Pinsky, B.L. J. Am. Chem. Soc. 1977, 99, 956.
50. Pittman, Jr., C.U.; Surynarayanan, J. Am. Chem. Soc. 1974, 96, 7916.
51. Wollman, R.G.; Hendrickson, D.N. Inorg. Chem. 1977, 16, 723.
52. Felton, R.H.; Owen, G.S.; Dolphin, D.; Forman, A.; Borg, D.C.; Fajer, J. Ann. N.Y. Acad. Sci. 1973, 206, 504.
53. Summerville, D.A.; Cohen, I.A. J. Am. Chem. Soc. 1976, 98, 1747.
54.a. Sacconi, L.; Mealli, C.; Gatteschi, D. Inorg. Chem. 1974, 13, 1985; b. Bencini, A.; Gatteschi, D.; Sacconi, L. Inorg. Chem. 1978, 17, 2670; c. Gatteschi, D.; Mealli, C.; Sacconi, L. Inorg. Chem. 1976, 15, 2774.
55. Gagné, R.R.; Koval, C.A.; Smith, T.J. J. Am. Chem. Soc. 1977, 99, 8367.
56. Gagné, R.R.; Koval, C.A.; Smith, T.J.; Cimolino, M.C. J. Am. Chem. Soc. 1979, 101, 4571.
57. Addison, A.W. Inorg. Nucl. Chem. Lett. 1976, 12, 899.
58. Weaver, T.R.; Meyer, T.J.; Adeyemi, S.A.; Brown, G.A.; Eckberg, R.P.; Hatfield, W.E.; Johnson, E.C.; Murray, R.W.; Untereker, D. J. Am. Chem. Soc. 1975, 97, 3039.
59. Phelps, D.W.; Kahn, E.M.; Hodgson, D.J. Inorg. Chem. 1975, 14, 2486.
60. Dunitz, J.D.; Orgel, L.E. J. Chem. Soc. 1953, 2594.
61. Bunker, B.C.; Drago, R.S.; Hendrickson, D.N.; Richman, R.M.; Kessell, S.L. J. Am. Chem. Soc. 1978, 100, 3805.

62. Kahn, O.; Tola, P.; Coudanne, H. Inorg. Chim. Acta 1978, 31, L405.
63. Kahn, O.; Tola, P.; Galy, J.; Coudanne, H. J. Am. Chem. Soc. 1978, 100, 3931.
64. Kahn, O.; Claude, R.; Coudanne, H. J. Chem. Soc. Chem. Comm. 1978, 1012.
65. Welo, L.A. Phil. Mag. 1928, [7], 6, 481.
66. Lupu, D. Rev. Roum. Chem. 1970, 15, 417.
67. Lupu, D.; Barb, D.; Filoti, G.; Morariu, M.; Tarina, D. J. Inorg. Nucl. Chem. 1972, 34, 2803.
68. Frisch, P.D.; Dahl, L.F. J. Am. Chem. Soc. 1972, 94, 5082.
69. Sorai, M.; Kosaki, A.; Suga, H.; Seki, S. Yoshida, T.; Otsuka, S. Bull. Chem. Soc. Japan 1971, 44, 2364.
70. Holm, R.H. Endeavour 1975, 34, 38.
71. Frankel, R.B.; Reiff, W.M.; Bernal, I.; Good, M.L. Inorg. Chem. 1974, 13, 493.
72. Wong, H.; Sedney, D.; Reiff, W.M.; Frankel, R.B.; Meyer, T.J.; Salmon, D. Inorg. Chem. 1978, 17, 194.
73. Neumann, M.A.; Trinh-Toan; Dahl, L.F. J. Am. Chem. Soc. 1972 94, 3383.
74. Frankel, R.B.; Reiff, W.M.; Meyer, T.J.; Cramer, J.L. Inorg. Chem. 1974, 13, 2515.
75a. Trinh-Toan; Teo, B.K.; Fergusson, J.A.; Meyer, T.J.; Dahl, L.F. J. Am. Chem. Soc. 1977, 99, 408; b. See, for example, Gall, R.S.; Chu, C.T.W.; Dahl, L.F. J. Am. Chem. Soc. 1974, 96, 4019.
76. Bertrand, J.A.; Hightower, T.C. Inorg. Chem. 1973, 12, 206.
77a. Petersen, J.L.; Schramm, C.S.; Stojakovic, D.R.; Hoffman, B.M.; Marks, T.J. J. Am. Chem. Soc. 1977, 99, 286; b. Schramm, C.J.; Stojakovic, D.R.; Hoffman, B.M.; Marks, T.J. Science 1978, 200, 47.
78. Hoffman, B.M.; Ibers, J.A.; Marks, T.J.; Scaringe, R.P.; Schramm, C.J.; Stojakovic, D.R. Symposium on Properties of Low Dimensional Solids, American Chemical Society National Meeting, Honolulu, Hawaii, April 2-5, 1979.
79. Hieber, H.; Lagally, H. Z. Anorg. Allg. Chem. 1940, 245, 321.
80. Fischer, E.O.; Brenner, K.S. Z. Naturforsch. B. 1962, 17, 774.
81. Krogmann, K.; Binder, W.; Hausen, H.D. Angew. Chem., Int. Ed. Engl. 1968, 7, 812; Angew. Chem. 1968, 80, 844.
82. Ginsberg, A.P.; Cohen, R.L.; DiSalvo, F.J.; West, K.W. J. Chem. Phys. 1974, 60, 2657.
83. Reis, Jr., A.H.; Hagley, V.S.; Peterson, S.W. J. Am. Chem. Soc. 1977, 99, 4184.
84. Alcácer, L.; Maki, A.H. J. Phys. Chem. 1974, 78, 215.
85. Alcácer, L.; Maki, A.H. J. Phys. Chem. 1976, 80, 1912.
86. Alcácer, L.; Novais, H.; Pedroso, F. In "Molecular Metals"; Hatfield, W.E., Ed.; Plenum: New York, 1979; p. 415.
87. Menth, A.; Rice, M.J. Solid State Comm. 1972, 11, 1025.
88. Krogmann, K.; Hausen, H.D. Z. Anorg. Allgem. Chem. 1968, 358, 67.

89. Kiundersma, P.I.; Sawatzky, G.A. Solid State Comm. 1973, 13, 39.
90. Phillips, J.C. Phys. Stat. Sol. 1977, 79B, 111.
91. Heitkamp, D.; Rade, H.S.; Keller, H.J.; Rupp, H.H. J. Solid State Chem. 1975, 15, 292.
92. Rudorff, W.; Schwarz, H.G.; Walter, M. Z. Anorg. Allg. Chem. 1952, 269, 141.
93. Brown, D.B.; Zubieta, J.A.; Valla, P.A.; Wrobleski, J.T.; Watt, T.; Hatfield, W.E.; Day, P. to be published.
94. Murphy, D.W.; DiSalvo, F.J.; Hull, Jr., G.W.; Waszczak, J.V.; Mayer, S.F.; Stewart, G.R.; Early, S.; Acrivos, J.V.; Geballe, T.H. J. Chem. Phys. 1975, 62, 967.
95. For a list of references, see Mayoh, B.; Day, P. J. Chem. Soc. Dalton Trans. 1976, 1483.
96. Mayoh, B.; Day, P. J. Chem. Soc. Dalton Trans. 1974, 846.
97. Beveridge, D.; Day, P. J. Chem. Soc. Dalton Trans. 1979, 648.
98. Herman, E.; Hanned, R.; Simkin, D.; Brand, D.E.; Muir, W.B. Canad. J. Phys. 1976, 54, 1149.
99. Walton, E.G.; Brown, D.B.; Wong, H.; Reiff, W.M. Inorg. Chem. 1977, 16, 2425.
100. Jones, Jr., E.R.; Hendricks, M.E.; Anel, T.; Amma, E.L. J. Chem. Phys. 1977, 66, 3252.
101. Walton, E.G.; Corvan, P.J.; Brown, D.B.; Day, P. Inorg. Chem. 1976, 15, 1737.
102. Chevrel, R.; Sergent, M.; Prigent, J. J. Solid State Chem. 1971, 3, 515.
103. Matthais, B.T. Science 1972, 175, 1465.
104. Fischer, Ø.; Odermatt, R.; Bongi, G.; Jones, H.; Chevrel, R.; Sergent, M. Phys. Lett. 1973, 45A, 87.
105. Fischer, Ø.; Treyvaud, A.; Chevrel, R.; Sergent, M. Solid State Comm. 1975, 17, 721.
106. Johnston, D.C.; Shelton, R.N. J. Low Temp. Phys. 1977, 26, 561.
107. McCallum, R.W.; Johnston, D.C.; Shelton, R.N.; Fertig, W.A.; Maple, M.B. Solid State Comm. 1977, 24, 501.
108. Dziobkowski, C.T.; Wrobleski, J.T.; Brown, D.B. to be published.
109. Herren, F.; Fischer, P.; Ludi, A.; Hälg, W. to be published.
110. Ito, A.; Suenaga, M.; Ono, K. J. Chem. Phys. 1968, 48, 3597.
111. Hush, N.S. Presentation at the NATO-ASI on "Mixed Valence Compounds", Oxford, England: September 15, 1979.

TECHNICAL REPORT DISTRIBUTION LIST, GEN

	No. Copies
Office of Naval Research 800 North Quincy Street Arlington, Virginia 22217 Attn: Code 472	2
ONR Branch Office 536 S. Clark Street Chicago, Illinois 60605 Attn: Dr. George Sandoz	1
ONR Branch Office 715 Broadway New York, New York 10003 Attn: Scientific Dept.	1
ONR Branch Office 1030 East Green Street Pasadena, California 91106 Attn: Dr. R. J. Marcus	1
ONR Area Office One Hallidie Plaza, Suite 601 San Francisco, California 94102 Attn: Dr. P. A. Miller	1
ONR Branch Office Building 114, Section D 666 Summer Street Boston, Massachusetts 02210 Attn: Dr. L. H. Peebles	1
Director, Naval Research Laboratory Washington, D.C. 20390 Attn: Code 6100	1
The Assistant Secretary of the Navy (R, E&S) Department of the Navy Room 4E736, Pentagon Washington, D.C. 20350	
Commander, Naval Air Systems Command Department of the Navy Washington, D.C. 20360 Attn: Code 310C (H. Rosenwasser)	1
Defense Documentation Center Building 5, Cameron Station Alexandria, Virginia 22314	12
U.S. Army Research Office P.O. Box 1211 Research Triangle Park, N.C. 27709 Attn: CRD-AA-IP	1
Naval Ocean Systems Center San Diego, California 92152 Attn: Mr. Joe McCartney	1
Naval Weapons Center China Lake, California 93555 Attn: Dr. A. B. Amster Chemistry Division	1
Naval Civil Engineering Laboratory Port Hueneme, California 93401 Attn: Dr. R. W. Drisko	1
Professor K. E. Woehler Department of Physics & Chemistry Naval Postgraduate School Monterey, California 93940	1
Dr. A. L. Slafkosky Scientific Advisor Commandant of the Marine Corps (Code RD-1) Washington, D.C. 20380	1
Office of Naval Research 800 N. Quincy Street Arlington, Virginia 22217 Attn: Dr. Richard S. Miller	1
Naval Ship Research and Development Center Annapolis, Maryland 21401 Attn: Dr. G. Bosmajian Applied Chemistry Division	1
Naval Ocean Systems Center San Diego, California 91232 Attn: Dr. S. Yamamoto, Marine Sciences Division	1

TECHNICAL REPORT DISTRIBUTION LIST, 053

	No. Copies
Dr. R. N. Grimes University of Virginia Department of Chemistry Charlottsville, Virginia 22901	1
Dr. M. Tsutsui Texas A&M University Department of Chemistry College Station, Texas 77843	1
Dr. M. F. Hawthorne University of California Department of Chemistry Los Angeles, California 90024	1
Dr. D. B. Brown University of Vermont Department of Chemistry Burlington, Vermont 05401	1
Dr. W. B. Fox Naval Research Laboratory Chemistry Division Code 6130 Washington, D.C. 20375	1
Dr. J. Adcock University of Tennessee Department of Chemistry Knoxville, Tennessee 39716	
Dr. W. Hatfield University of North Carolina Department of Chemistry Chapel Hill, North Carolina 27514	1
Dr. D. Seyferth Massachusetts Institute of Technology Department of Chemistry Cambridge, Massachusetts 02139	1
Dr. M. H. Chisholm Department of Chemistry Indiana University Bloomington, Indiana 47401	1
Dr. B. Foxman Brandeis University Department of Chemistry Waltham, Massachusetts 02154	1
Dr. T. Marks Northwestern University Department of Chemistry Evanston, Illinois 60201	1
Dr. G. Geoffrey Pennsylvania State University Department of Chemistry University Park, Pennsylvania 16802	1
Dr. J. Zuckerman University of Oklahoma Department of Chemistry Norman, Oklahoma 73019	1
Professor O. T. Beachley Department of Chemistry State University of New York Buffalo, New York 14214	1
Professor P. S. Skell Department of Chemistry The Pennsylvania State University University Park, Pennsylvania 16802	1
Professor K. M. Nicholas Department of Chemistry Boston College Chestnut Hill, Massachusetts 02167	;